Preliminary Report
of
The Hakuhō Maru Cruise KH-75-5

September 12 - October 27, 1975
Kuroshio and Adjacent Waters

Ocean Research Institute
University of Tokyo
1978

Preliminary Report
of
The Hakuhō Maru Cruise KH-75-5

September 12 - October 27, 1975
Kuroshio and Adjacent Waters

By
The Scientific Members of the Expedition
Edited by
Toshihiko Teramoto

1978

Contents

1 Introduction

This cruise was laid out in the three legs. The first leg (Leg I) aimed at observing behaviours of the Kuroshio in the area where the Kuroshio crossed over the Izu Ridge. A special interest was taken in revealing the changes in movements of surface and subsurface waters of the Kuroshio. The changes in the movements of waters were supposed to be generated in close association with the change in density stratification. The tracking of the movements was carried out by the use of surface and subsurface drogues. The STD sectioning was made in parallel for obtaining an information on the structure of density stratification. The second leg (Leg II) aimed at presenting the detailed density structure of the Kuroshio to the south of Japanese Islands. Besides, the Eulerian measurements of velocity were made by means of arrays of currentmeters at several subsurface layers in the Kuroshio and the vicinal coastal regions. The Kuroshio had formed the large meander since May of the year of this cruise, so observations were focussed to make clear the linked structure of the Kuroshio with the accompanying large cold eddy. The third leg (Leg III) aimed at revealing the fine density structure formed in association with the presence of the small sea mount, Kokushosone. Temperature profilings were carried out with XBT at a short interval in a area around the sea mount. During the period of these observations on the three legs, additional observations and water samplings were made in parallel for the other purposes described in the section 3.4.

After finishing the observations, the ship called at the port of the International Ocean Exposition in Okinawa to keep open house to general visitors to the Exposition.

2 Personnel

TERAMOTO, Toshihiko (Chief Scientist)	Ocean Research Institute, University of Tokyo (1-15-1, Minamidai, Nakano-ku, Tokyo 164)	P.O.
MAEDA, Akio	"	"
TAIRA, Keisuke	"	"
WATANABE, Masaaki	"	"
SHIKAMA, Nobuyuki	"	"
NAKAI, Toshisuke	"	O.
OTOBE, Hirotaka	"	"
KOIZUMI, Kinichiro	"	Gp.
SAINO, Toshiro	"	Bc.
NAGATA, Yutaka	Geophysical Institute, University of Tokyo (2-11-16, Yayoi, Bunkyo-ku, Tokyo 113)	P.O.
FUKASAWA Masao	"	"
ISHII, Haruo	Geophysical Institute, Tohoku University (Aoba, Aramaki, Sendai-shi 980)	"
SUZUKI, Yoshimitu	"	"
TANIYA, Masazumi	"	"
TAKANO, Kenzo	Institute of Physical and Chemical Research (2-1, Hirosawa, Wako-shi, Saitama 351)	"
OKAZAKI, Moriyoshi	"	"
MATSUIKE, Kanau	Tokyo University of Fisheries (4-5-7, Kounan, Minato-ku, Tokyo 108)	O.P.
KUNISHI, Hideaki	Geophysical Institute, Kyoto University (Kitashirakawaoiwake, Sakyo-ku, Kyoto-shi 606)	P.O.
IMAWAKI, Shiro	"	"
ODAMAKI, Minoru	"	"
HARASHIMA, Akira	"	"
ENDO, Shuichi	"	"
MORINAGA, Tsutomu	Department of Fishery, Kinki University (3-4-1, Kowakae, Higashioosaka-shi 577)	O.P.
SAKURAI, Masahito	Faculty of Technology, Kagoshima University (1-21-40, Koorimoto, Kagoshima-shi 890)	P.O.

Speciality
P.O.: Physical Oceanography. G.: Geophysics. Bc.: Biochemistry.
O.: Oceanography. O.P.: Optical Oceanography.

3 Observations

3.1 Leg I Tracking of the Kuroshio with drifters

by N. Shikama and T. Teramoto

It is evident from past observations that the flow of the Kuroshio in the area to the south of Japanese Islands extend to the depth more than 1000 m. We have no knowledge, however, on how the Kuroshio behaves in the area where the Kuroshio cross over the Izu Ridge. The water depth of the area is less than 1000 m except for the narrow trough to the south of Mikurajima. For revealing the behaviours of the Kuroshio in the area, the tracking of surface and subsurface drogues was tried. Fig. 3.1.1 shows a schematic configuration of a drifting system with a subsurface drogue. As shown in the figure, a parachute for sea-anchoring a fishing boat is used as a drogue. Three drifting systems of this type were deployed. Lengths of piano wires used to connect the subsurface drogues with surface buoys of the three systems were choosen to be 300, 700 and 1000 m, respectively. The systems were launched near the axis of the Kuroshio to the west of the Izu Ridge. A surface drogue was also launched. To all of these drifting systems radar transponders with different frequencies were attached. The tracking of these systems was made by the help of ship's radar. During the tracking of the drogues, cross-stream sectionings with XBT and STD were made.

The drifting systems with subsurface drogue did not work well unfortunately. The 300 m-, 700 m and 1000 m-drogue systems submerged 18 hrs, 4 hrs and 15 hrs after their launching, respectively. Since a depth gauge installed at the 700 m - drogue

could not be recovered, an information on behaviour of the drifting system with subsurface drogue is not available unfortunately. The malfunction of these systems is seemed to be attributed to the descending tendency in the movements of the sea-anchore parachutes during their driftings. Such a tendency could not be suspected from the configuration of the parachutes and from several-hours operations of the similar systems deployed for operational test in the cruise of the R/V Tanseimaru conducted in May, 1975.

The result of the tracking is illustrated in Figs. 3.1.2 and 3.1.3. In these figures, distributions of surface velocity obtained through dead-reckoning were presented. XBT and STD sections along lines illustrated in Fig. 3.1.4 are shown in Figs. 3.1.5, 3.1.6, 3.1.7 and 3.1.8.

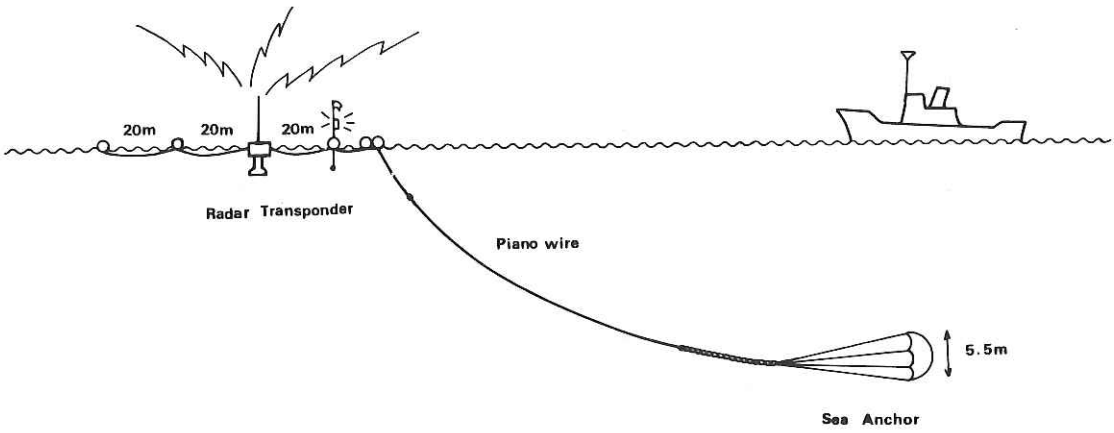

Fig. 3.1.1 Configuration of a drifting system with subsurface drogue.

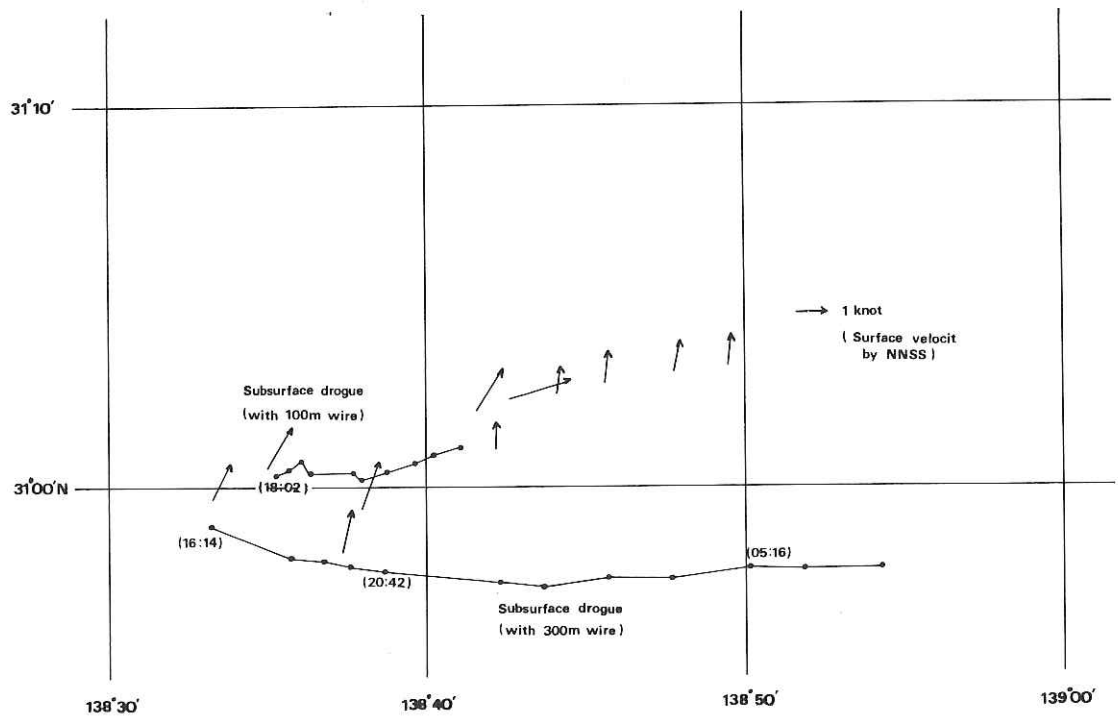

Fig. 3.1.2 Results of tracking from 15 to 16 Sept. 1975.

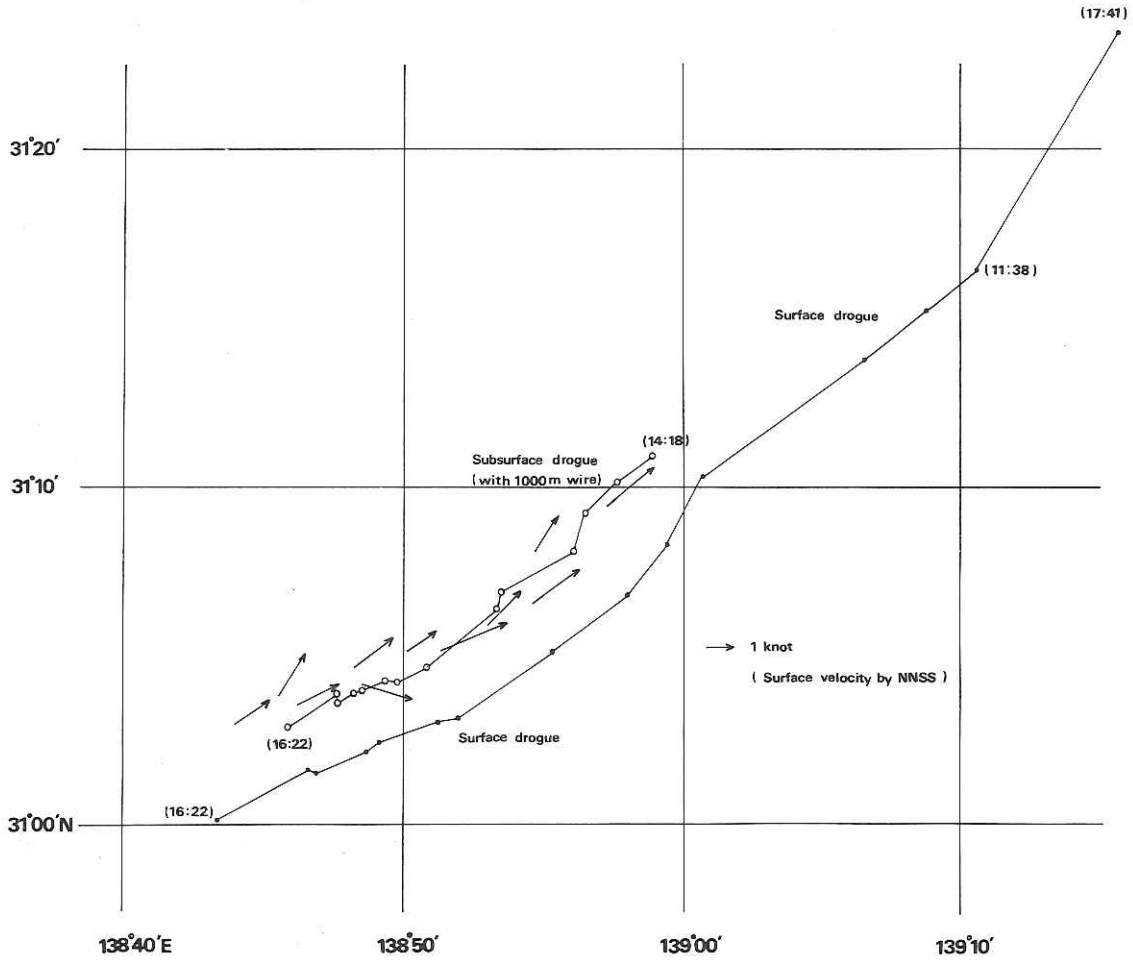

Fig. 3.1.3 Results of tracking from 17 to 18 Sept. 1975.

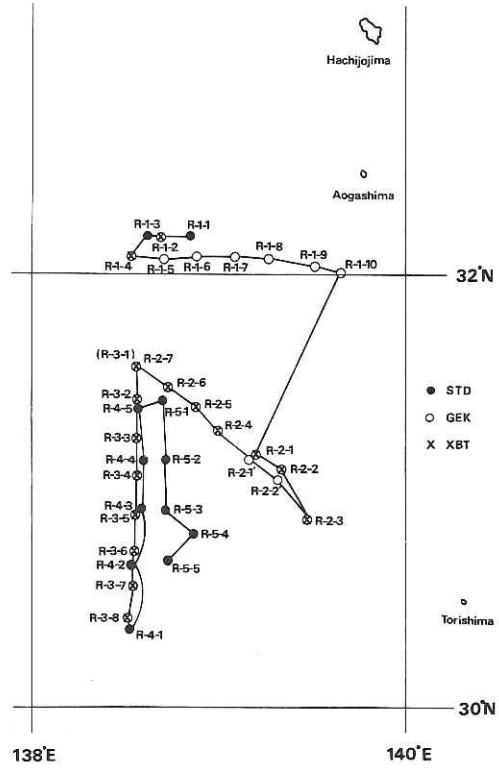

Fig. 3.1.4 Lines of sectioning STD and XBT.

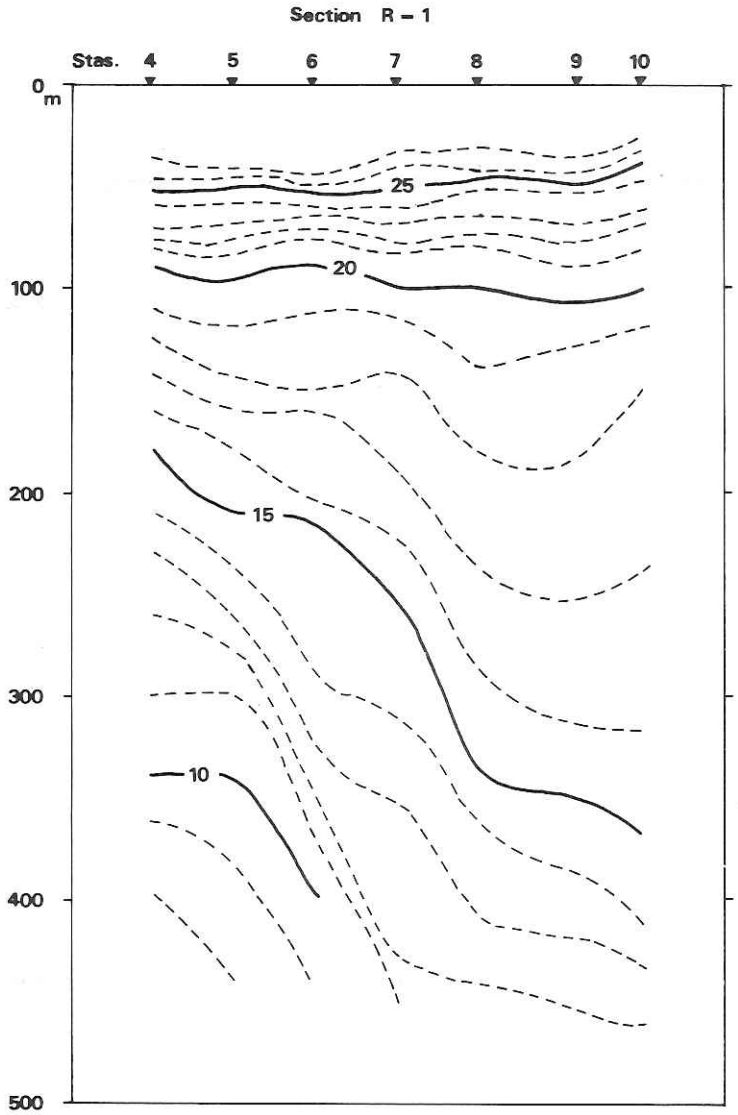

Fig. 3.1.5 A temperature section along R-1.

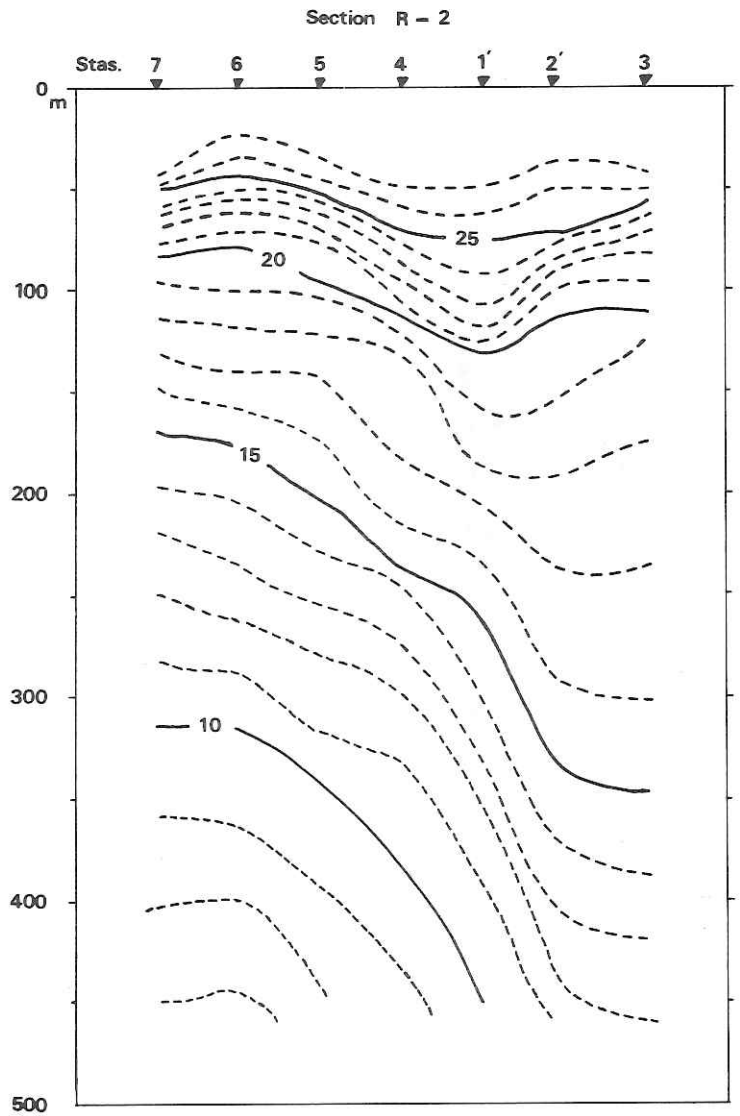

Fig. 3.1.6 A temperature section along R-2.

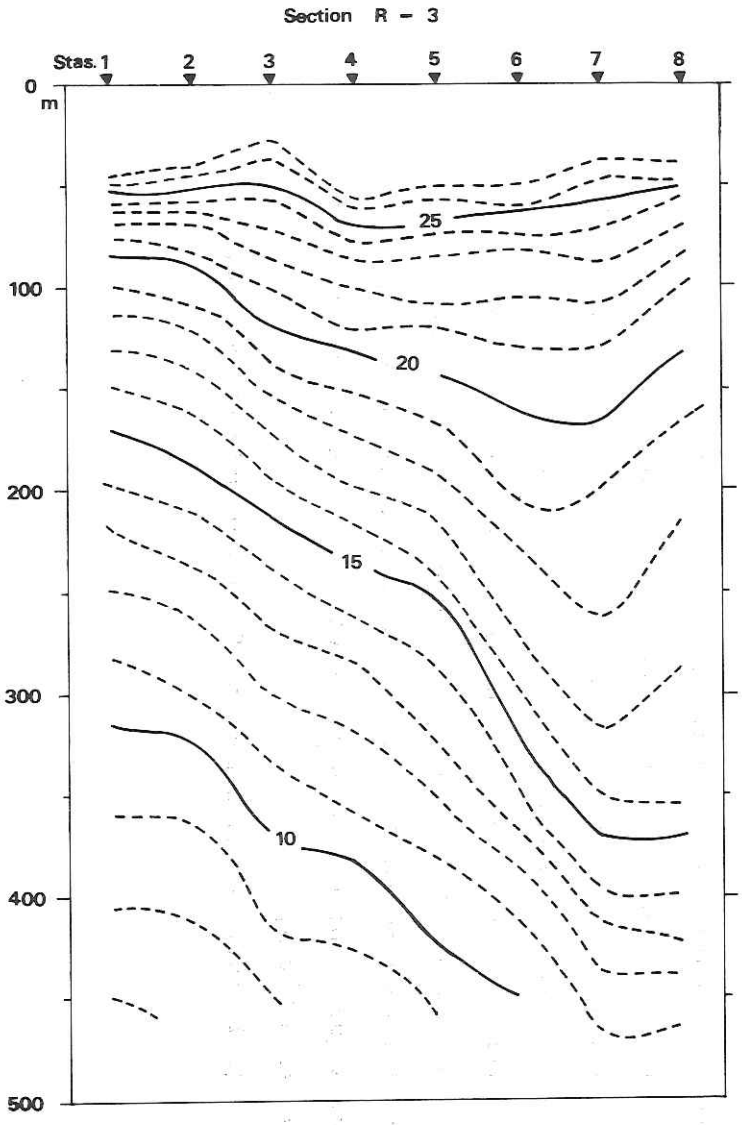

Fig. 3.1.7 A temperature section along R-3.

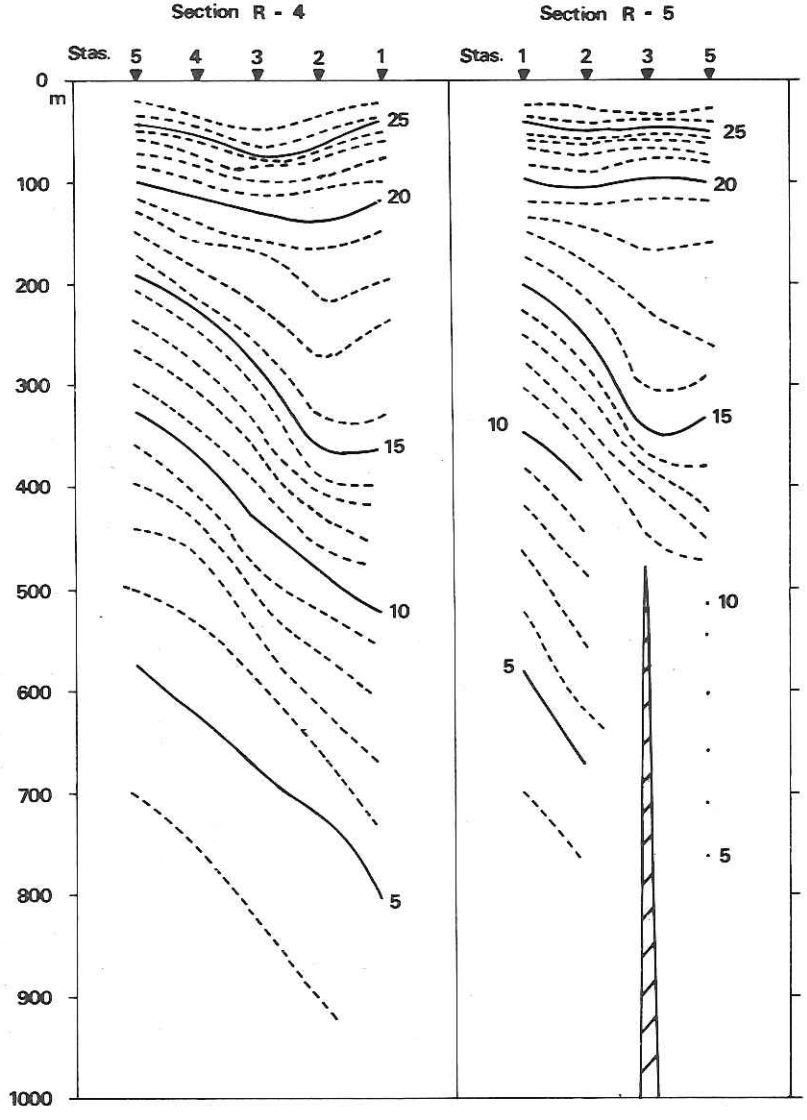

Fig. 3.1.8 A temperature section along R-4.

3.2 Leg II Observations of density structure and measurements of currents in the Kuroshio and adjacent regions

3.2.1 General description of the leg II

by H. Kunishi

It is well-known that there are two stable paths for the Kuroshio south of Japan. One is a slope path, which remains above the continental slope off Enshunada. The other is a meander path, which leaves the continental slope off Shikoku and meanders off Enshunada. Since 1963 the Kuroshio has flowed along the slope path. From May to Angust in 1975, however, a meander pattern of the Kuroshio east of Kyushu moved to the east and developed to a large meander with a cold water region off Enshunada. It was expected early in September that the meander would become the stationary meander.

In the leg II were made some observations to understand the horizontal and vertical structures of the Kuroshio with a stationary meander south of Japan. They are;

(i) a tracking of the Kuroshio from Murotomisaki to Irozaki by XBT and GEK, which is described in the section 3.2.2,

(ii) two cross sections of the Kuroshio off Shikoku and off Enshunada by STD and hydrographic casts, which are described in the section 3.2.2. They are also analyzed from a viewpoint of a quasi-absolute pressure field, which is described in the section 3.2.5,

(iii) current measurements of the Kuroshio off Shikoku by

moored current meters, which are described in the section 3.2.3,

(iv) several short sections of the Kuroshio off Shikoku and off Enshunada by BT, XBT and GEK, which are described in the section 3.2.2, and

(v) continuous surface temperature and salinity measurements on board the ship, which are described in the section 3.2.2, current measurements on the continental shelf off Shikoku by moored current meters, which are described in the section 3.2.4, and optical measurements of the Kuroshio water, which are described in the section 3.4.1.

Figure 3.2.1 shows the ship track and positions of stations in the leg II.

The Kuroshio continued to flow along the meander path for at least ten months. Therefore, these observations could be regarded as observations of the Kuroshio in the early stage of the stationary meander.

3.2.2 Tracking and cross sections of the Kuroshio with a meander

by H. Kunishi, S. Imawaki, M. Odamaki, A. Harashima, S. Endo, M. Okazaki and S. Nakai

A tracking and several cross sections of the Kuroshio were made to understand the structures of the Kuroshio with a stationary meander. Observations performed are listed in Table 3.2.1. A tracking TRK was aimed to give the horizontal flow pattern of the Kuroshio at the beginning of the observations. According to the result of TRK was decided the position of the section MEN in the meander region. A long cross section SIK off Shikoku was provided because it seemed to be suitable for a monitoring section of the Kuroshio in the upstream side of the meander region. The other long cross section MEN off Enshunada was provided to observe the vertical structure of the Kuroshio in the western half of the meander region, where the ocean floor is fairly flat and as deep as 4,000 m. It could be compared with the section SIK, where the Kuroshio flows usually on the continental slope.

After the leg I an intercalibration of current meters was made at a station (32°N, 136°E) on Sep. 19. Then cross sections KI1 and KI2 were made to grasp the situation of the Kuroshio southeast to Shikoku. Short cross sections SI1 and SI2 off Shikoku were also made. The mooring MB was deployed on Sep. 21. A short section AS1 was performed on the way to the mooring

station MA. After the deployment of the mooring MA the long cross section SIK off Shikoku by STD and hydrographic casts was begun on Sep. 22 from Station S-1 toward the south. Station spacing of STD lowering was 6 miles in the strong current region of the Kuroshio and 20-30 miles in the south of the region. At Station S-9, however, some trouble happened on the STD wintch. Hence the cross section was stopped and it was decided to call at the Port Shimizu and repair the wintch. On the way to Shimizu was performed a tracking TRK of the Kuroshio by XBT and GEK, where strong horizontal gradients of 200 m temperature (14-17^{o}C) and relatively large GEK surface velocities are considered to be the indicators of the Kuroshio.

After the repair of the STD wintch a cross section IZ1 by BT was made along the west side of the Izu-Ogasawara Ridge. The cross section MEN off Enshunada by STD and hydrographic casts was started on Sep. 28 from Station M-1 toward the west-southwest. Station spacing of STD lowering was 10 miles in the strong current region of the Kuroshio. Intercalibration among STD, BT, XBT, DBT, and hydrographic casts was done at Station M-2. Because of the rough weather condition on Sep. 30 were abandoned STD lowerings at Stations from M-13 to M-15, where only DBT observations were made. The cross section SIK was started again on Oct. 1 from the southernmost station S-28 toward the north. All the observations were carried out satisfactorily until Oct. 4. But before the end of the section the Tyhoon 7513, Cora ap-

proached to the observation area. It was decided that the section SIK was stopped at Station S-9-2, which is the same position of Station S-9 on Sep. 23, and the retrieval of the mooring MB should be tried on Oct. 4 advancing by one day. After a partly retrieval of the mooring MB and a perfect retrieval of MA a short XBT section SI3 was made from MA to MB on Oct. 6.

Surface temperature and salinity were measured continuously during the cruise by two surface TS meters, which were able to measure the temperature and salinity of the pumped-up sea water under way.

The STD was Hytech Model 9006 with a 1500 m depth sensor, which had nominal precisions of 3.75 m for depth, 0.02°C for temperature and 0.02 for salinity. Hydrographic casts at several stations provided the calibration data for the STD records. The STD was lowered to 1500 m depth. In the lower part of the deep hydrographic casts were used protected reversing thermometers of range -1° to 3°C, graduated at intervals of 0.02°C, which were expected to give temperatures accurate to within 0.01°C. Salinities from the hydrographic cast were determined on the Auto-Lab indicative salinometer, Model 601 Mk. III, which had a nominal precision of $\pm$0.003 . Dissolved oxygens were determined by the Winkler method.

A result of the tracking TRK is shown in Fig. 3.2.2, where the horizontal distribution of 200 m temperature is shown by contours and GEK surface velocities are illustrated by arrows.

Dotted lines indicate the ship track. One of the remarkable features is an approach of the Kuroshio to Shionomisaki in spite of the period of the stationary meander.

Temperature section of SIK measured by STD is shown in Fig. 3.2.3. It consists of two parts, which are drawn in separate panels. The left-hand side panel was observed seven days ahead to the right-hand side one, and hence they should not be connected simply. Strong temperature gradient in the upper layer between Stations S-7 and S-9 is remarkable. Figure 3.2.4 shows the geostrophic velocity section of SIK, which was calculated from the STD data and refered to the bottom or 1500 db surface. The strong current region of the Kuroshio is located between Stations S-7 and S-20. Comparing the present Kuroshio with the Kuroshio without a meander, velocities are relatively weak but the width is relatively large. And some stripes of relatively strong currents are recognized. Temperature, salinity and disolved oxygen sections of SIK measured by hydrographic casts are shown in Figs. 3.2.5, 3.2.6 and 3.2.7, respectively. The horizontal temperature gradient in the deep water between Stations S-15 and S-25 is in the same direction as that in the upper layer, which implies the existence of geostrophic velocity of the Kuroshio near to the bottom.

In Fig. 3.2.8 is shown the temperature section of MEN measured by STD and DBT. Station M-2 is located at the center of the cold water region off Enshunada. Strong temperature gra-

dient between Station M-6 and M-7 is noticeable. The geostrophic velocity section of MEN is shown in Fig. 3.2.9, which was calculated from the STD data and refered to 1500 db surface. The strong current region of the Kuroshio is located between Stations M-5 and M-10, and it is devided into two strong current parts by a relatively weak current between Stations M-7 and M-8. In this section is also seen a stripe-like feature of strong currents in the Kuroshio. It is recognized from the hydrographic data of Stations M-6 and M-9 that the horizontal temperature gradient of the Kuroshio penetrates near to the bottom of 4000 m depth. It indicates that the geostrophic velocity of the Kuroshio extends near to the bottom.

Geostrophic volume transports of the Kuroshio are estimated in several cases from STD and hydrographic data, which are tabulated in Table 3.2.2. In the table the upper figures are the total geostrophic transports over 1000 db surface, which are refered to as upper transports for convenience. The lower figures are those refered to the bottom and integrated from the sea surface to the bottom, which are refered to as total transports. The upper transport of the Kuroshio with a meander is a little smaller than that without a meander. The total transport of the Kuroshio with a meander, however, is not smaller than that without a meander. These facts suggest that the deep water also should be observed for the discussion on the transports of the Kuroshio in relation to the stationary meander.

In conclusion, comparing the present Kuroshio with a meander with the Kuroshio without a meander current speed is relatively weak, the width of the Kuroshio is relatively wide and the penetration of the current is relatively deep.

Results of the hydrographic casts are tabulated in Table 3.2.3 to 3.2.11, where observed quantities are presented on the left-hand side and interpolated and calculated quantities are on the right-hand side.

Table 3.2.1. List of a tracking and cross sections performed in the leg II.

Section	Duaration	Measurements*
KI1	Sep. 19-20	XBT, GEK
KI2	Sep. 20	XBT, GEK
SI1	Sep. 20-21	GEK
SI2	Sep. 20-21	DBT
AS1	Sep. 21-22	BT, GEK
SIK	Sep. 22-23, Oct. 1-4	STD, Hydro., XBT, GEK
TRK	Sep. 23-26	XBT, GEK
IZ1	Sep. 27-28	DBT
MEN	Sep. 28-30	STD, Hydro., DBT, GEK
SI3	Oct. 6	XBT

* DBT indicates Bathythermograph for the deep water (1000 m) and Hydro. indicates hydrographic casts.

Table 3.2.2. Geostrophic volume transports of the Kuroshio, expressed in a unit of 10^6 m^3/sec.

	with meander		without meander
	Shikoku*	Enshunada**	Shikoku***
upper transpot	51	56	68
total transport	75	102	88

* Between Stations S-6 and S-28 of the present cruise of Hakuho Maru (1975)

** Between Stations M-2 and S-25 of the present cruise (1975)

*** Between Stations 841 and 857 of Atlantis II (1965)

Table 3.2.3

KH-75-5 Sta. S-7, 32°48.7'N, 133°49.6'E, Sept. 22 1975, 1908 GMT, Depth 1080 m, Wave -2, Wind S 2.5 m/s, Bar 1012.8 mb, Air Temp. 26.4°C.

D(m)	T(°C)	S(‰)	O_2(ml/ℓ)	D(m)	T(°C)	S(‰)	D($^{dyn.}_{m}$)
0	27.2	33.523	4.64	0	27.2	33.523	0.0
25	24.36	34.270	4.30	20	24.93	34.121	0.114
50	19.78	34.642	4.42	50	19.78	34.642	0.242
75	18.16	34.678	3.98	75	18.16	34.678	0.322
100	17.29	34.662	3.99	100	17.29	34.662	0.394
150	14.63	34.613	3.81	150	14.63	34.613	0.521
200	13.10	34.513	3.54	200	13.10	34.513	0.629
300	10.17	34.367	3.08	300	10.17	34.367	0.814
400	8.21	34.283	2.79	400	8.21	34.283	0.968
500	6.91	34.260	2.40	500	6.91	34.260	1.102
600	5.83	——	2.08	600	5.83	34.260	1.222
700	5.05	34.288	1.83	700	5.05	34.288	1.330
800	4.20	34.348	1.61	800	4.20	34.348	1.425
900	3.68	34.399	1.54	1000	3.31	34.435	1.586
1000	3.31	34.435	1.60				

Table 3.2.4

KH-75-5 Station M-2, 32°28.3'N, 138°05.2'E, Sep. 28. 1975, 0224 and 0425 GMT, Depth 3961 m, Wave -3, Wind NNE-7.0 m/s, Bar 1015.0 mb, Air Temp. 26.1°C.

D(m)	T(°C)	S(‰)	O_2(ml/ℓ)	D(m)	T(°C)	S(‰)	D($\frac{dyn}{m}$·)
0	27.2	33.651	4.61	0	27.2	33.651	0.0
25	27.12	33.644	4.62	20	27.14	33.645	0.123
49	22.48	34.322	4.44	50	22.32	34.339	0.279
73	19.22	34.567	3.96	75	19.00	34.575	0.374
98	16.89	34.605	3.78	100	16.77	34.606	0.448
147	14.44	34.568	3.70	150	14.25	34.561	0.571
196	11.50	34.446	3.45	200	11.34	34.440	0.672
294	8.73	34.346	2.69	300	8.59	34.341	0.829
391	6.77	34.291	2.37	400	6.59	34.287	0.960
489	5.11	34.268	1.93	500	4.99	34.271	1.070
587	4.32	34.313	1.57	600	4.24	34.323	1.164
685	3.81	34.378	1.49	700	3.77	34.381	1.249
782	3.62	34.390	1.46	800	3.57	34.396	1.328
978	2.99	34.464	1.51	1000	2.93	34.471	1.473
1172	2.54	34.517	1.81	1200	2.49	34.525	1.598
1324A	2.31	34.556	1.90	1500	2.15	34.579	1.766
1467	2.17	34.575	2.13	2000	1.836	34.630	2.014
1527A	2.13	34.582	2.18	2500	1.657	34.663	2.243
1731A	1.973	34.606	2.41	3000	1.538	34.678	2.462
1935A	1.866	34.626	2.58	3500	1.501	34.686	2.678
2140A	1.777	34.639	2.77				
2550A	1.643	34.666	3.01				
2756A	1.589	34.669	3.15				
2961A	1.546	34.677	3.32				
3167A	1.510	34.680	3.37				
3372A	1.505	34.685	3.39				
3576A	1.501	34.687	3.46				
3779A	1.522	34.689	3.47				
3961A	1.527						

A) Cast II.

Table 3.2.5

KH-75-5 Sta. M-6, 32°09.6'N, 137°27.8'E, Sept. 28, 1975, 2032 GMT, Depth 4100 m, Wave -3, Wind SW 5.0 m/s, Bar 1012.3 mb, Air Temp. 27.0°C.

D(m)	T(°C)	S(‰)	O_2(ml/ℓ)	D(m)	T(°C)	S(‰)	D($\frac{dyn}{m}$·)
1286	2.49	34.534	1.99	1500	2.21	34.573	——
1487	2.22	34.571	2.19	2000	1.828	34.630	——
1688	2.072	34.595	2.38	2500	1.620	34.657	——
1889	1.899	34.621	2.63	3000	1.497	34.681	——
2090	1.781	34.636	2.78	3500	1.500	34.684	——
2292	1.694	34.646	2.96				
2495	1.621	34.657	3.14				
2698	1.566	34.669	3.18				
2901	1.508	34.678	3.30				
3105	1.493	34.682	3.43				
3310	1.499	34.682	3.47				
3515	1.500	34.684	3.51				
3721	1.516	34.683	3.51				
3979	1.522	34.686	3.56				

Table 3.2.6

KH-75-5 Station M-9, 31°58.8'N, 136°55.2'E, Sep. 29. 1975, 0828 GMT, Depth 4250 m, Wave -2, Wind - 5.0 m/s, Bar 1010.8 mb, Air Temp. 26.4°C.

D(m)	T(°C)	S(‰)	O_2(ml/ℓ)	D(m)	T(°C)	S(‰)	D($\frac{dyn}{m}$·)
1281	2.73	34.504	1.71	1500	2.44	34.541	——
1479	2.46	34.537	1.90	2000	1.920	34.616	——
1678	2.248	34.572	2.20	2500	1.672	34.655	——
1876	2.025	34.601	2.45	3000	1.520	34.675	——
2074	1.869	34.624	2.68	3500	1.500	34.686	——
2272	1.770	34.644	2.82	4000	1.535	34.686	——
2471	1.682	34.653	3.04				
2670	1.620	34.664	3.12				
2870	1.547	34.672	3.35				
3068	1.512	34.677	3.39				
3269	1.509	34.682	3.66A				
3517	1.500	34.686	3.49				
3767	1.523	34.685	3.54				
4067	1.538	34.686	3.54				

A) Uncertain Value

Table 3.2.7

KH-75-5 Station S-27, 30°26.2'N, 134°42.0'E, Oct. 1. 1975, 0020 and 0245 GMT, Depth 4620 m, Wave -5, Wind ENE-12.0 m/s, Bar 1014.5 mb, Air Temp. 27.1°C.

D(m)	T(°C)	S(‰)	O_2(ml/ℓ)	D(m)	T(°C)	S(‰)	D($\frac{dyn}{m}$·)
0	38.2	34.337	4.43	0	28.2	34.337	0.0
21	28.19	34.311	4.43	20	28.19	34.312	0.120
42	28.17	34.311	4.40	50	27.24	34.374	0.295
63	25.44	34.517	4.65	75	24.31	34.675	0.423
83	23.70	34.772	4.50	100	22.90	34.841	0.531
125	22.16	34.840	4.36	150	21.31	34.857	0.726
165	20.82	34.861	4.34	200	19.77	34.856	0.900
247	18.56	34.831	4.26	300	17.55	34.793	1.203
328	17.10	34.769	4.32	400	16.01	34.709	1.474
408	15.88	34.701	4.27	500	14.05	34.562	1.717
490	14.27	34.577	4.00	600	11.68	34.410	1.929
571	12.44	34.456	3.70	700	9.23	34.282	2.109
815	6.74	34.194	2.53	800	7.05	34.202	2.259
985A	4.80	34.271B	1.73	1000	4.73	34.271	2.496
993	4.77	34.266	1.69	1200	3.70	34.377	2.683
1243	3.48	34.394	1.37	1500	2.78	34.487	2.908
1439A	2.91	34.471	1.41	2000	2.125	34.591	3.206
1628A	2.56	34.517	1.68	2500	1.811	34.635	3.460
1865A	2.253	34.572	2.10	3000	1.636	34.666	3.694
2102A	2.045	34.602	2.42	3500	1.527	34.679	3.918
2340A	1.901	34.624	2.63	4000	1.547	34.684	4.142
2579A	1.772	34.640	2.84	4500	1.592	34.687	4.376
2818A	1.689	34.660	3.02				
3059A	1.620	34.667	3.11				
3302A	1.551	34.674	3.34				
3547A	1.526	34.680	3.38				
3794A	1.543	34.688B	3.42				
4044A	1.548	34.684	3.50				
4295A	1.577	34.685	3.49				
4548A	1.596	34.687	3.43				

A) Cast II.

B) Uncertain value

Table 3.2.8

KH-75-5 Station S-25, 31°08.7'N, 134°30.9'E, Oct. 1. 1975, 1145 and 1358 GMT, Depth 4600 m, Wave -5, Wind ENE-13.0 m/s, Bar 1014.6 mb, Air Temp. 26.3°C.

D(m)	T(°C)	S(‰)	O_2(ml/ℓ)	D(m)	T(°C)	S(‰)	D($\frac{dyn}{m}$·)
0A	28.0	34.211	4.51	0	28.0	34.211	0.0
24A	28.03	34.199	4.54	20	28.03	34.201	0.120
48A	27.34	34.376	4.78	50	27.18	34.398	0.295
72A	25.18	34.628	4.69	75	24.94	34.650	0.425
96A	23.50	34.765	4.44	100	23.31	34.776	0.538
144A	21.80	34.834	4.43	150	21.62	34.843	0.737
192A	20.47	34.889	4.61	200	20.25	34.887	0.916
288A	17.98	34.809	4.37	300	17.74	34.800	1.227
384A	16.11	34.716	4.45	400	15.78	34.691	1.498
478A	14.03	34.556	4.14	500	13.48	34.516	1.735
572A	11.58	34.390	3.66	600	10.80	34.347	1.937
666A	9.08	34.263	3.32	700	8.35	34.233	2.106
760A	7.24	34.199	2.80	800	6.62	34.195	2.248
949A	4.86	34.244	1.77	1000	4.42	34.283	2.476
1139A	3.63	34.390	1.43	1200	3.43	34.416	2.652
1184	3.49	34.409	1.44	1500	2.64	34.514	2.863
1372	2.88	34.484	1.64	2000	2.271	34.572	3.162
1430A	2.75	34.499	1.70	2500	1.852	34.632	3.426
1610	2.528	34.532	1.89	3000	1.629	34.656	3.662
1849	2.383	34.554	2.05	3500	1.550	34.678	3.888
2088	2.198	34.584	2.24	4000	1.553	34.682	4.114
2328	1.966	34.616	2.63				
2569	1.814	34.637	2.79				
2810	1.694	34.652	2.98				
3050	1.616	34.657	3.23				
3291	1.565	34.674	3.31				
3532	1.549	34.678	3.41				
3774	1.533	34.679	3.47				
3966	1.553	34.682	3.49				
4160	1.555	34.681	3.35				

A) Cast II.

Table 3.2.9

KH-75-5 Station S-22, 31°34.8'N, 134°21.3E, Oct. 2. 1975, 0035 and 0242 GMT, Depth 4550 m, Wave -4, Wind SE-8.0 m/s, Bar 1014.7 mb, Air Temp. 26.7°C.

D(m)	T(°C)	S(‰)	O_2(ml/ℓ)	D(m)	T(°C)	S(‰)	D($\frac{dyn}{m}$·)
0A	27.9	34.054	4.53	0	27.9	34.054	0.0
25A	27.72	34.033	4.54	20	27.76	34.037	0.121
50A	26.47	34.241	4.44	50	26.47	34.241	0.295
75A	24.73	34.558	4.29	75	24.73	34.558	0.424
100A	23.42	34.689	4.35	100	23.42	34.689	0.538
150A	20.91	34.750	4.18	150	20.91	34.750	0.737
200A	19.39	34.816	4.35	200	19.39	34.816	0.909
299A	16.79	34.747	4.38	300	16.77	34.746	1.203
399A	14.66	34.605	4.20	400	14.64	34.603	1.455
498A	12.22	34.428	3.84	500	12.17	34.425	1.673
597A	9.92	34.297	3.46	600	9.85	34.294	1.860
696A	7.74	34.214	2.88	700	7.67	34.213	2.017
794A	6.16	34.208	2.31	800	6.08	34.209	2.151
991A	4.36	34.290	1.56	1000	4.31	34.295	2.368
1187A	3.55	34.403	1.45	1200	3.50	34.411	2.542
1231	3.40	34.428	1.46	1500	2.74	34.500	2.759
1430	2.87	34.484	1.63	2000	2.079	34.597	3.050
1479A	2.78	34.495	1.67	2500	1.773	34.649	3.298
1678	2.453	34.542	1.94	3000	1.579	34.669	3.526
1928	2.143	34.589	2.27	3500	1.526	34.679	3.748
2176	1.951	34.615	2.52	4000	1.549	34.683	3.973
2424	1.810	34.646	2.78				
2673	1.697	34.654	3.10				
2922	1.598	34.667	3.19				
3171	1.551	34.673	3.34				
3419	1.525	34.678	3.43				
3668	1.534	34.685B	3.48				
3916	1.540	34.682	3.49				
4164	1.568	34.684	3.51				
4413	1.584	34.683	3.49				

A) Cast II.

B) Uncertain value

Table 3.2.10

KH-75-5 Station S-18, 32°00.1'N, 134°12.1'E, Oct. 2. 1975, 1617 and 1821 GMT, Depth 4480 m, Wave -3, Wind S-8.0 m/s, Bar 1012.3 mb, Air Temp. 26.4°C.

D(m)	T(°C)	S(‰)	O_2(ml/ℓ)	D(m)	T(°C)	S(‰)	D($\frac{dyn}{m}$·)
0	27.8	34.069	4.51	0	27.8	34.069	0.0
25	27.82	34.054	4.49	20	27.82	34.057	0.121
50	27.41	34.264	4.51	50	27.41	34.264	0.299
75	25.71	34.449	4.37	75	25.71	34.449	0.436
100	24.08	34.642	4.04	100	24.08	34.642	0.557
149	20.42	34.827	4.21	150	20.38	34.828	0.756
199	19.20	34.803	4.55	200	19.17	34.802	0.922
299	16.48	34.694	4.09	300	16.45	34.693	1.213
398	13.92	34.554	4.05	400	13.86	34.550	1.457
498	11.17	34.366	3.69	500	11.12	34.363	1.662
597	8.90	34.244	3.37	600	8.84	34.243	1.835
695	7.18	34.241	2.57	700	7.09	34.239	1.981
793	5.59	34.210	2.15	800	5.51	34.212	2.105
988	4.10	34.332	1.54	1000	4.04	34.340	2.308
1181	3.32	34.433	1.58	1200	3.26	34.438	2.471
1277A	3.02	34.457	1.57	1500	2.60	34.515	2.676
1473	2.62	34.510	1.78	2000	2.026	34.599	2.959
1474A	2.64	34.509	1.78	2500	1.746	34.643	3.206
1719A	2.310	34.558	2.06	3000	1.583	34.667	3.434
1965A	2.052	34.595	2.40	3500	1.519	34.678	3.656
2211A	1.897	34.621	2.70	4000	1.547	34.681	3.881
2456A	1.765	34.641	2.91				
2702A	1.670	34.653	3.21				
2948A	1.595	34.665	3.30				
3193A	1.546	34.672	3.37				
3439A	1.517	34.677	3.48				
3684A	1.531	34.679	3.49				
3930A	1.537	34.680	3.54				
4127A	1.562	34.683	3.53				
4274A	1.561	34.683	3.57				

A) Cast II.

Table 3.2.11

KH-75-5 Station S-15, 32°14.7'N, 134°06.0'E, Oct. 3. 1975, 0423 and 0640 GMT, Depth 2850 m, Wave -3, Wind SSW-11.0 m/s, Bar 1008.0 mb, Air Temp. 27.6°C.

D(m)	T(°C)	S(‰)	O_2(ml/ℓ)	D(m)	T(°C)	S(‰)	D($\frac{dyn}{m}$·)
0	28.2	34.026	4.71	0	28.2	34.026	0.0
25	27.79	34.005	4.54	20	27.87	34.009	0.123
50	27.52	34.058	4.52	50	27.52	34.058	0.304
75	26.59	34.298	4.45	75	26.59	34.298	0.448
100	24.32	34.631	4.42	100	24.32	34.631	0.576
150	21.00	34.825	4.24	150	21.00	34.825	0.779
200	18.73	34.822	4.39	200	18.73	34.822	0.946
299	16.46	34.740	4.41	300	16.42	34.737	1.228
397	12.58	34.457	4.30	400	12.49	34.451	1.460
495	10.00	34.308	3.50	500	9.87	34.300	1.647
592	7.90	34.218	3.05	600	7.80	34.225	1.803
689	6.83	34.309	1.97B	700	6.63	34.305	1.936
785	5.16	34.262	1.86	800	5.00	34.263	2.050
891	4.28	34.294	1.60	1000	3.68	34.356	2.237
1120	3.28	34.427	1.46	1200	3.11	34.455	2.392
1259A	3.01	34.472	1.55	1500	2.53	34.531	2.589
1452A	2.60	34.521	1.85	2000	1.955	34.615	2.865
1694A	2.289	34.565	2.12	2500	1.647	34.655	3.097
1935A	2.037	34.603	2.48				
2176A	1.764	34.641	2.85				
2417A	1.679	34.651	2.99				
2657A	1.587	34.664	3.17				

A) Cast II.

B) Uncertain value

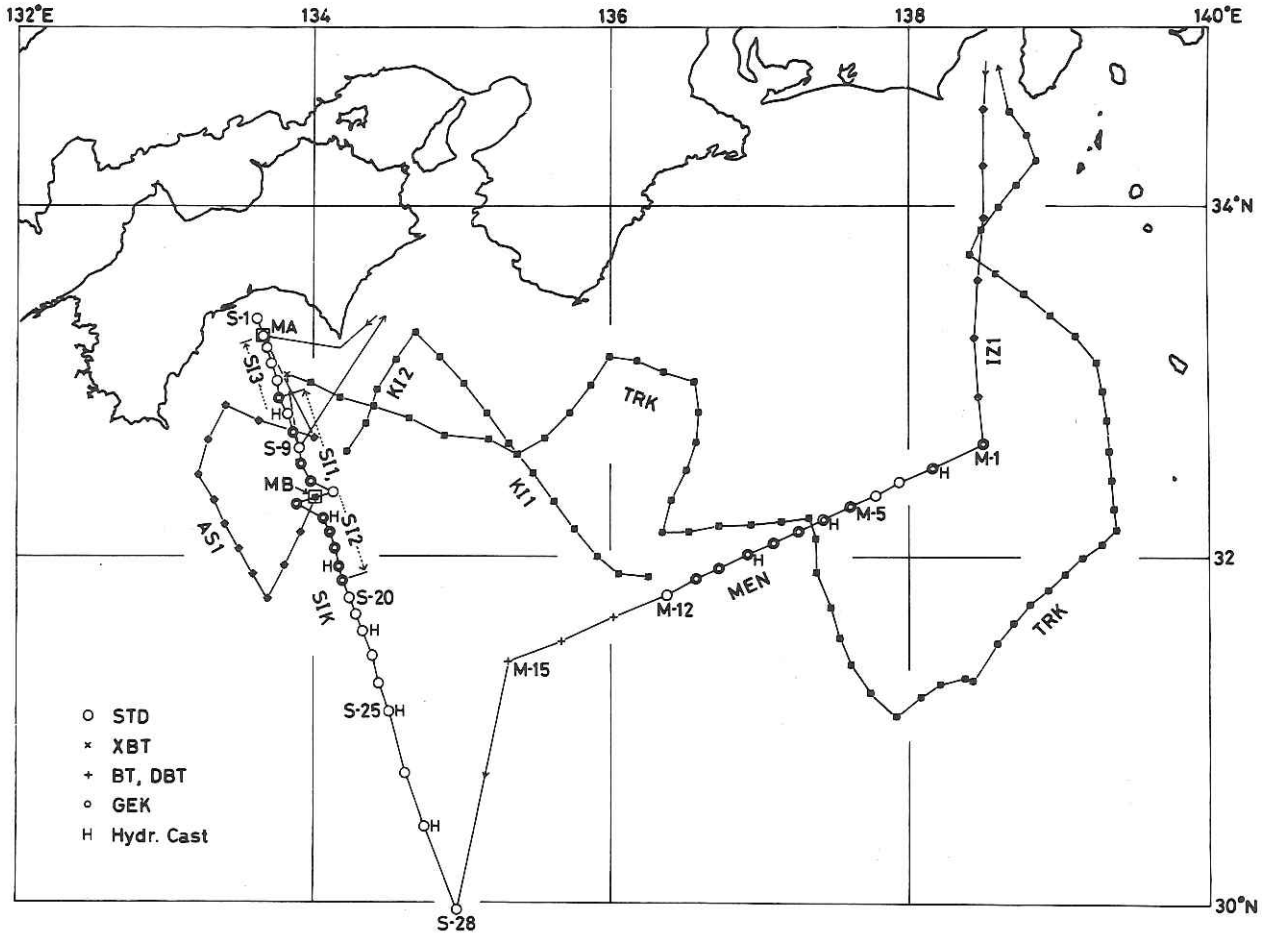

Fig. 3.2.1 Ship track and positions of stations in the Leg II.

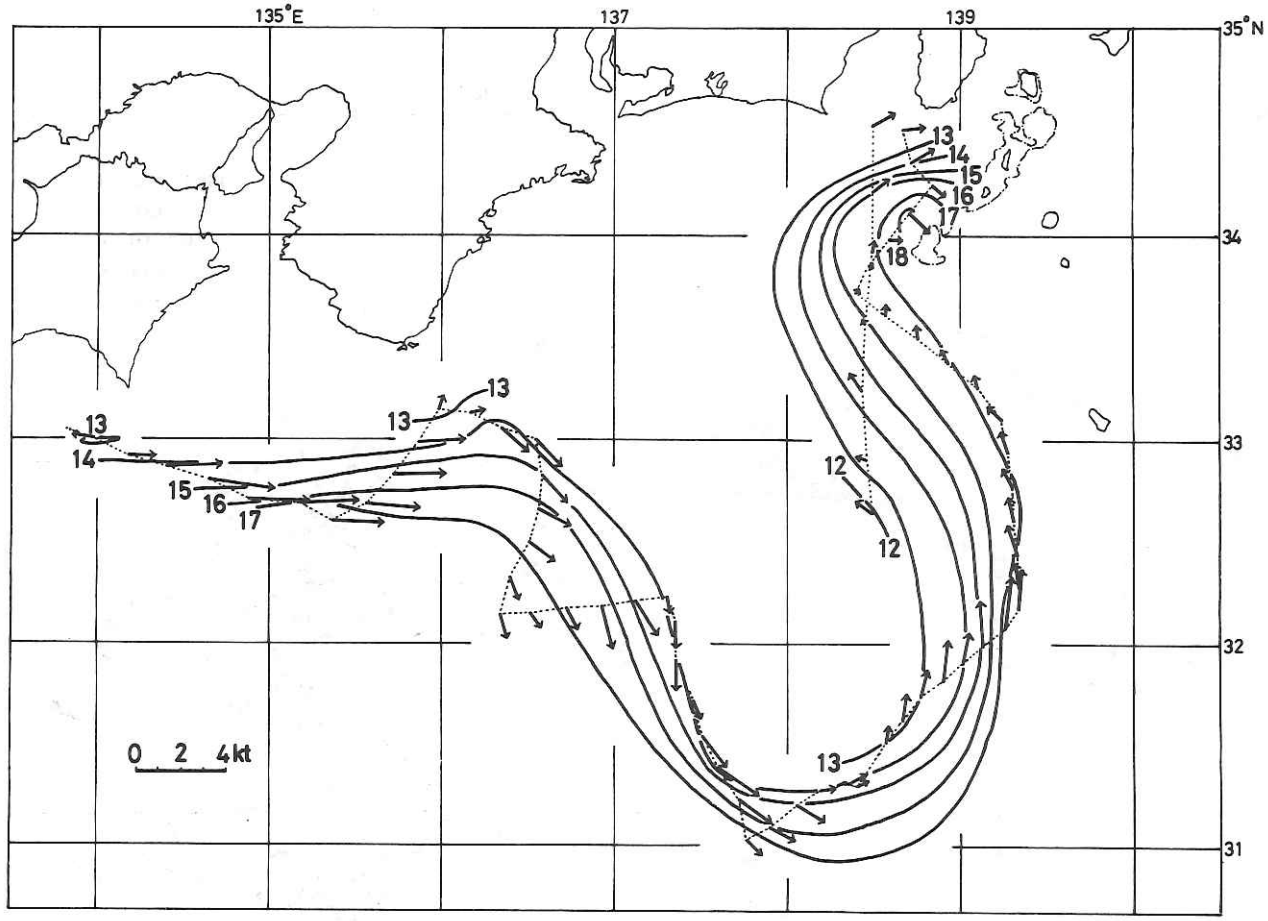

Fig. 3.2.2 Horizontal distribution of 200 m temperature and GEK surface velocities obtained by TRK. Isotherms are labeled in °C. Arrows indicate GEK velocities.

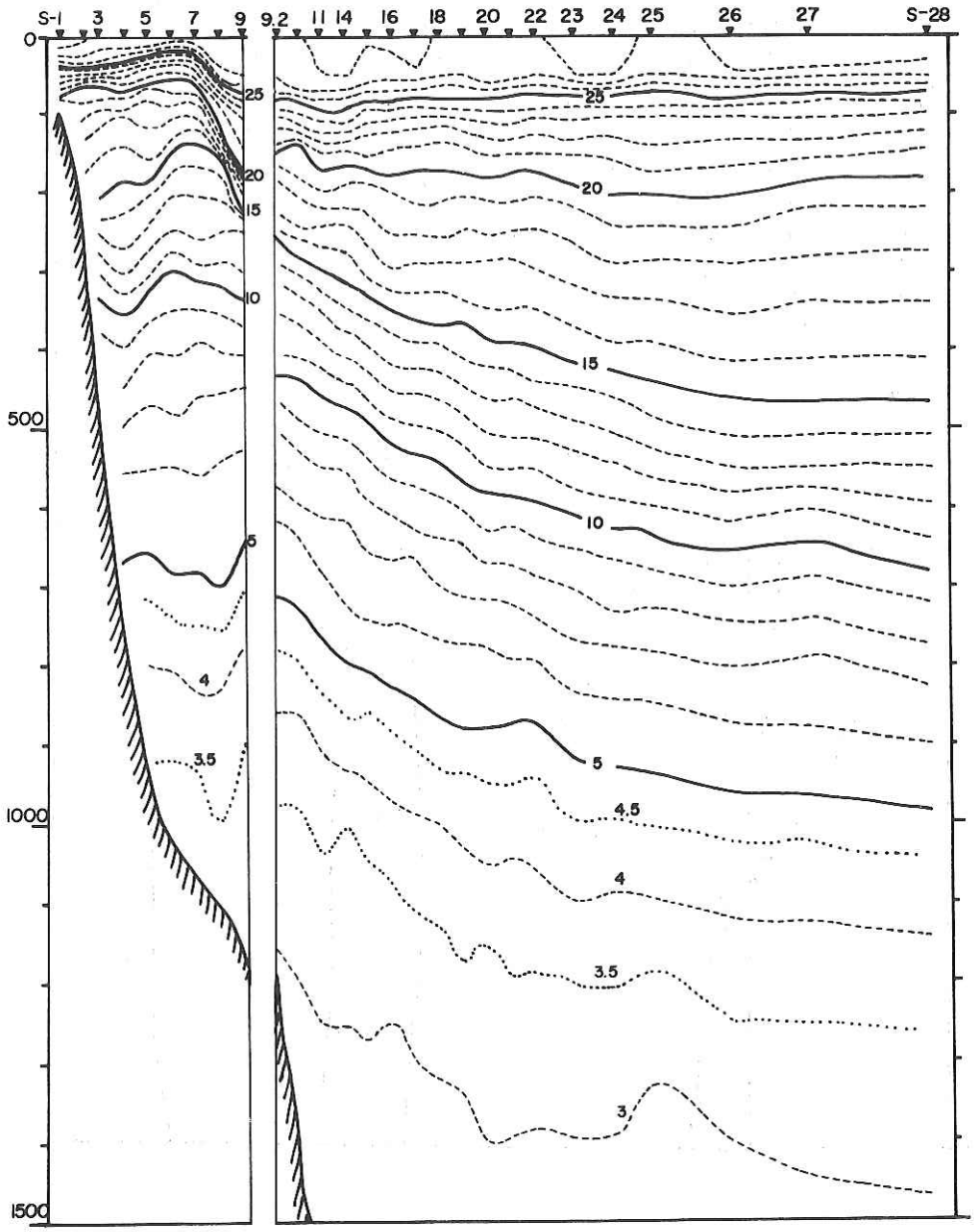

Fig. 3.2.3 Temperature section of SIK measured by STD. Vertical exaggeration is 1:371.

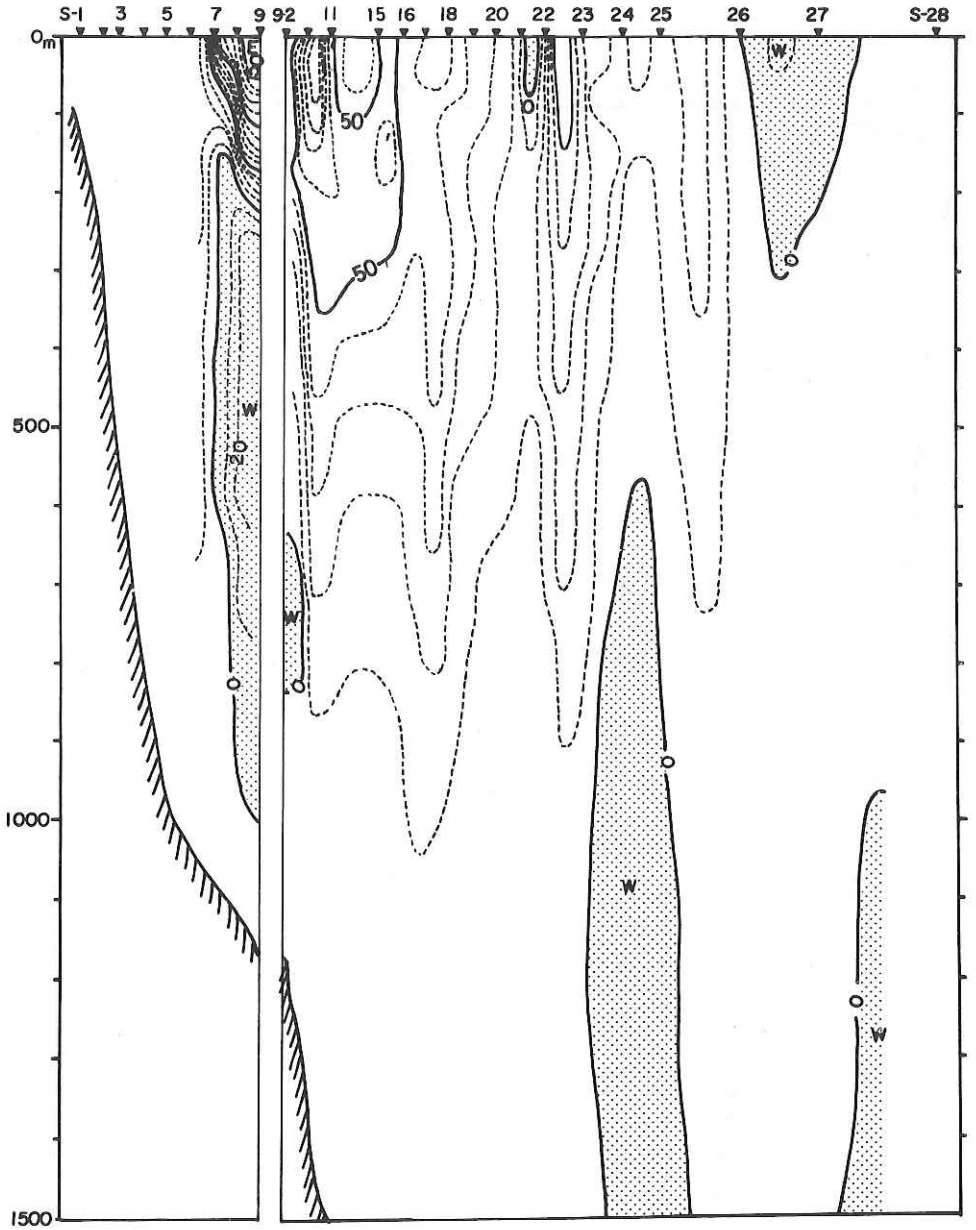

Fig. 3.2.4 Geostrophic velocity section of SIK calculated from STD data and refered to 1500 db. Isotaches are labeled in cm/sec; positive indicates eastward flow and negative (shaded part) westward flow.

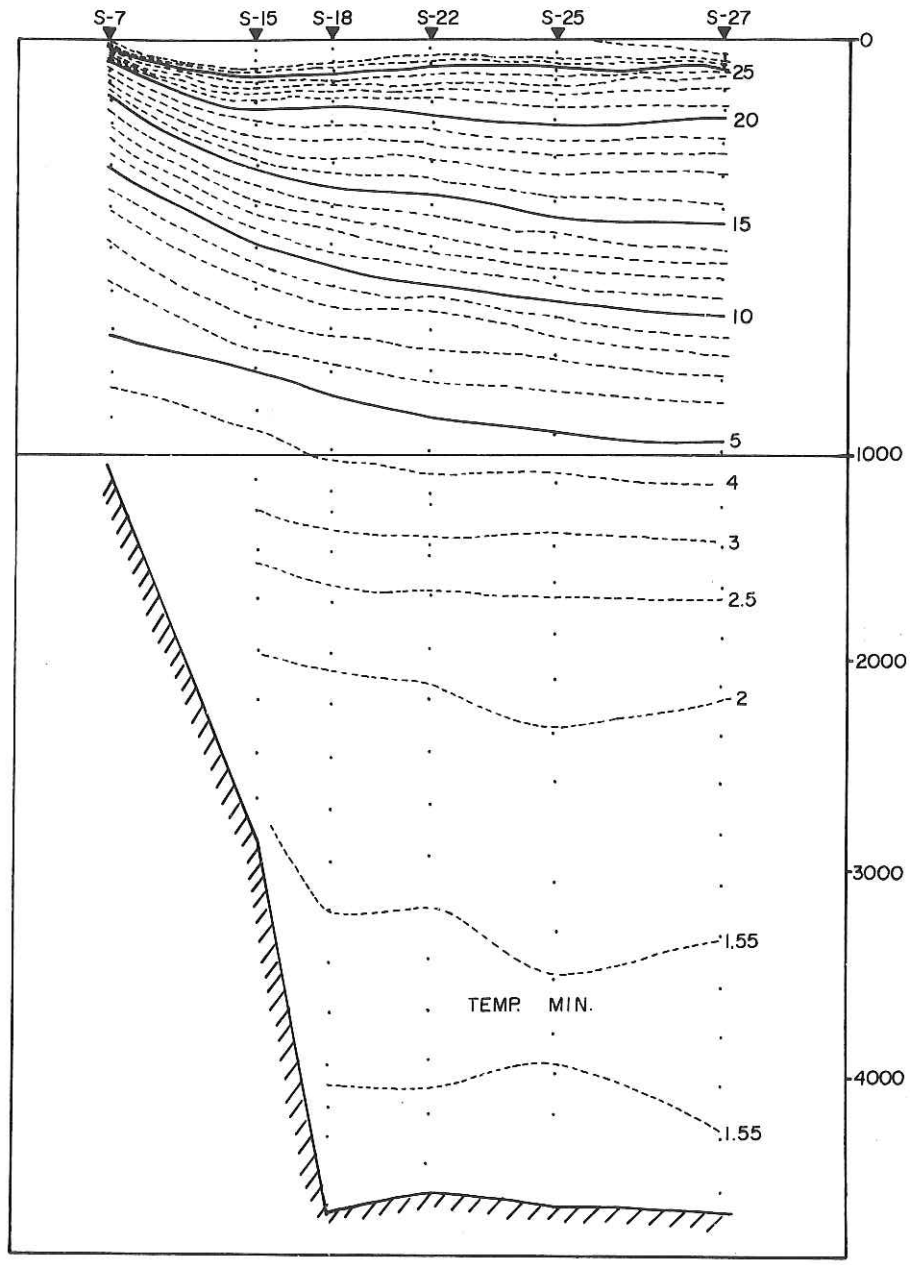

Fig. 3.2.5 Temperature section of SIK measured by hydrographic casts. Vertical exaggeration is 1:185 above 1000 m depth and 1:93 below 1000 m.

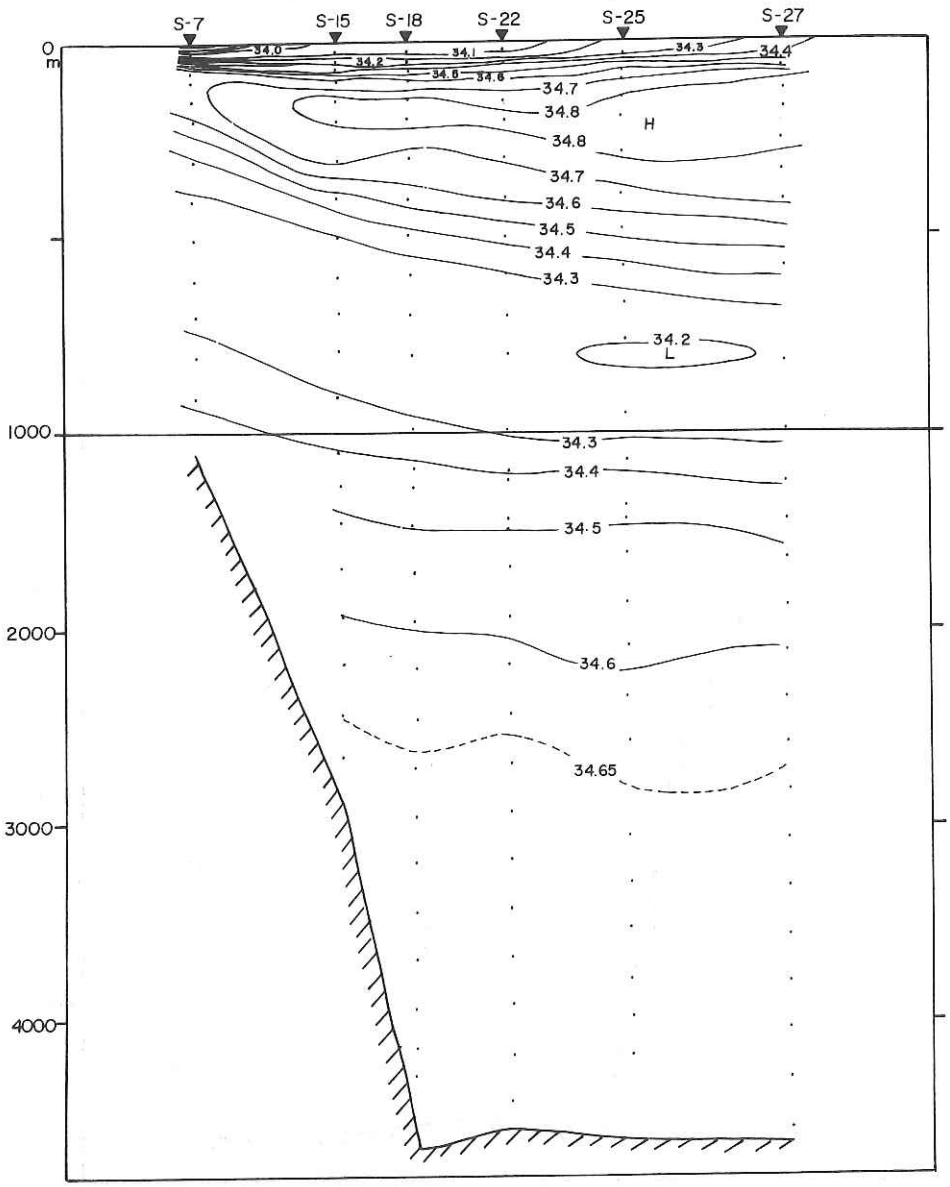

Fig. 3.2.6 Salinity section of SIK measured by hydrographic casts.

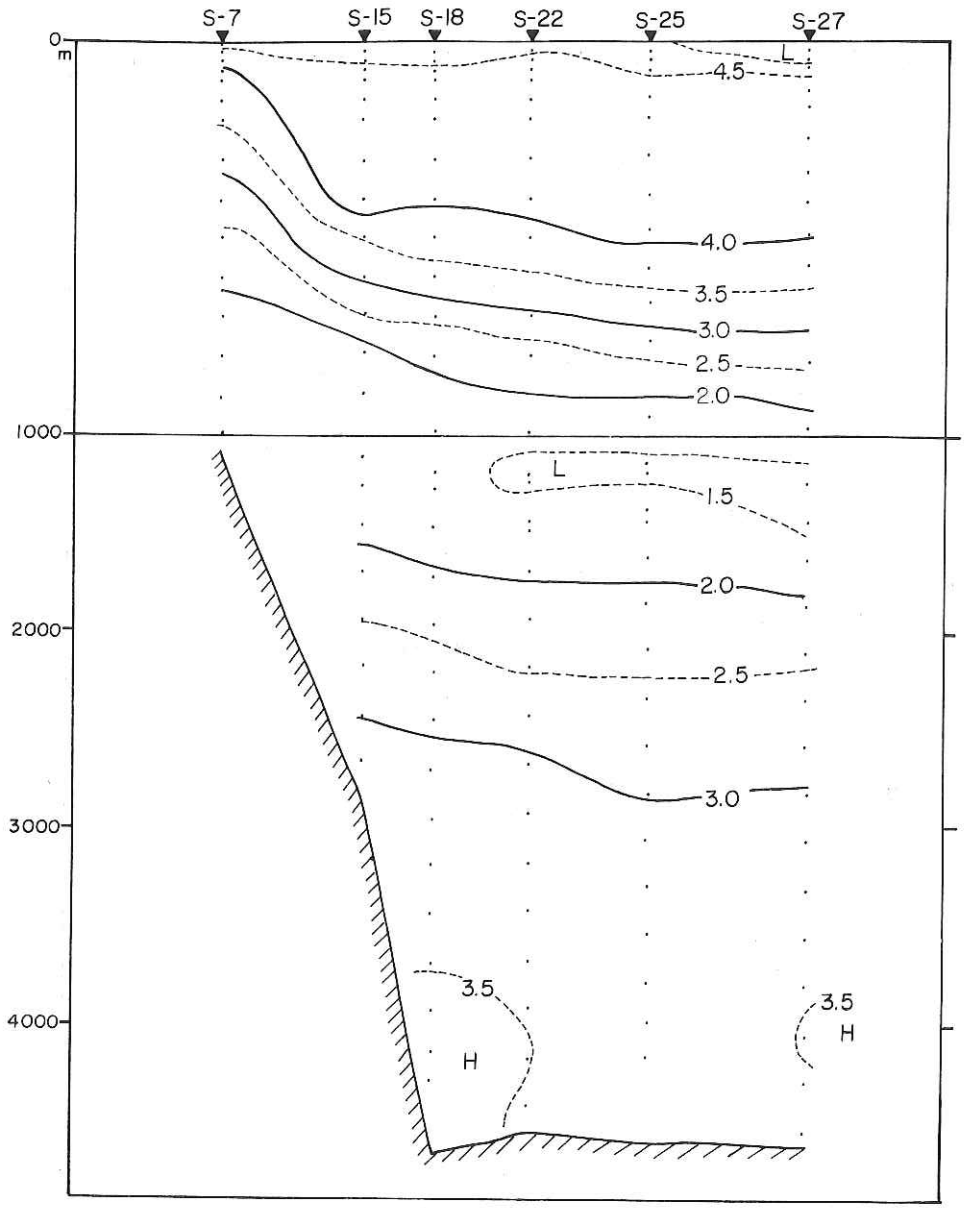

Fig. 3.2.7 Dissolved oxygen section of SIK measured by hydrographic casts.

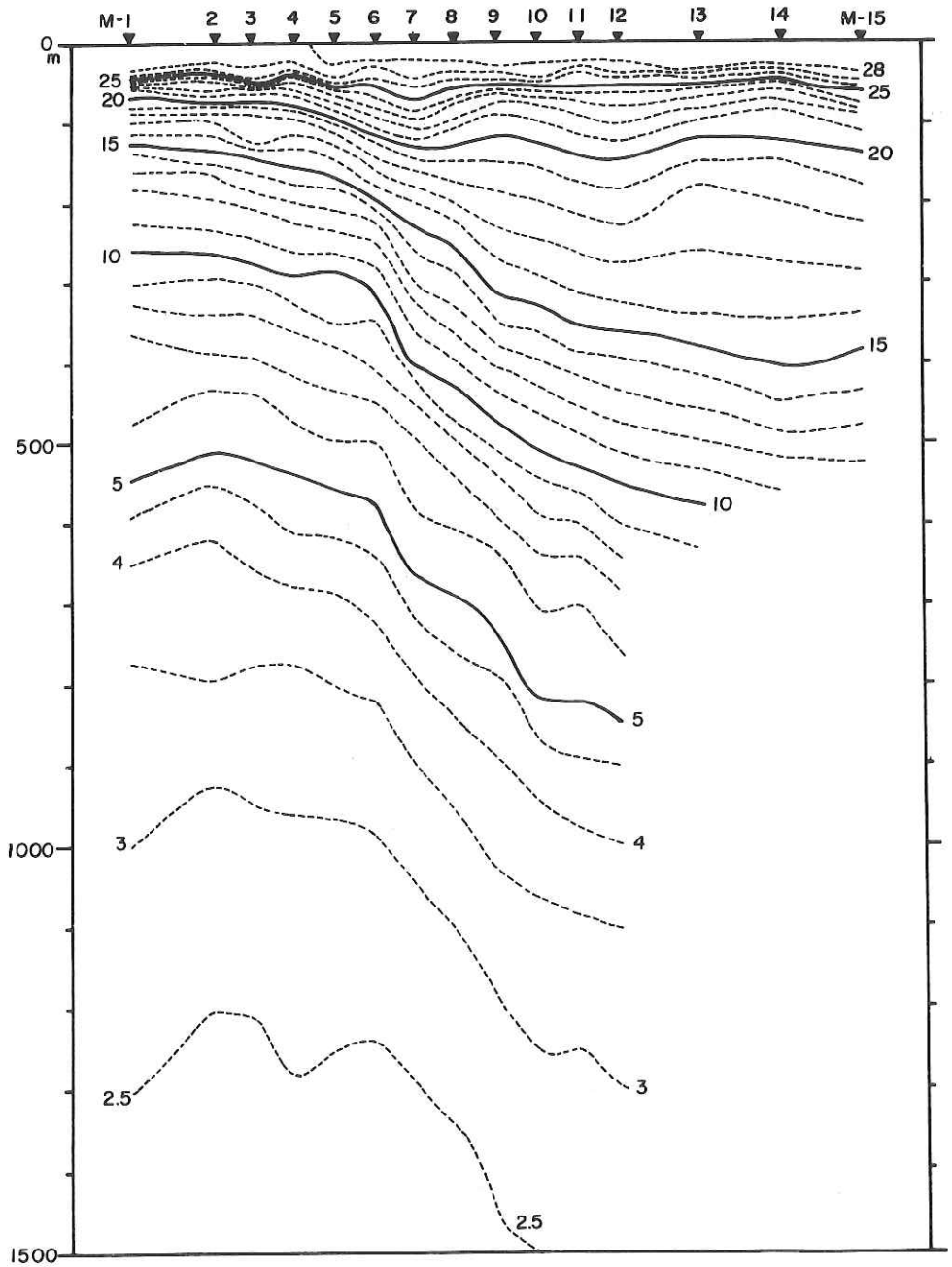

Fig. 3.2.8 Temperature section of MEN measured by STD and DBT in a part. Vertical exaggeration is 1:371.

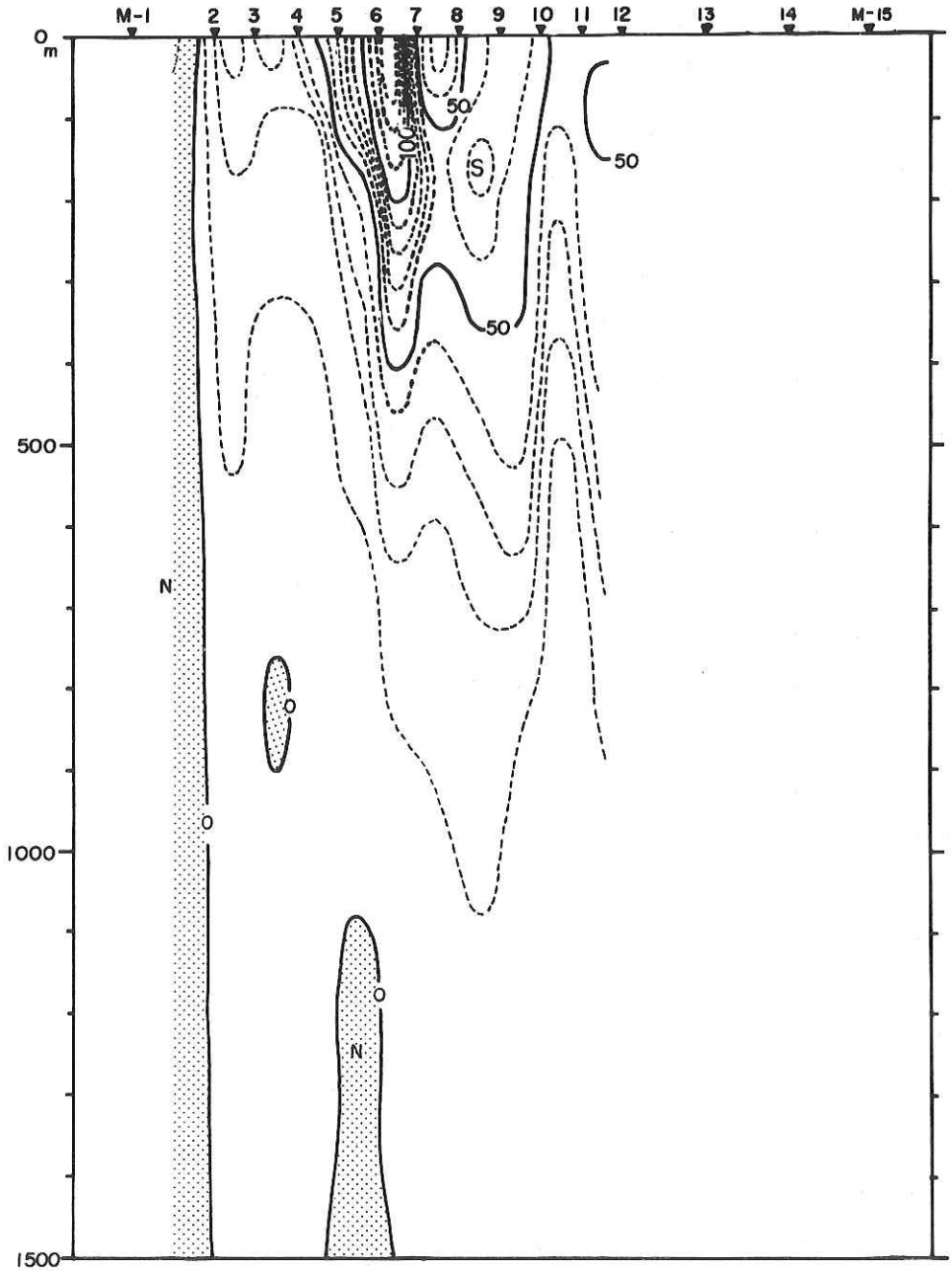

Fig. 3.2.9 Geostrophic velocity section of MEN calculated from STD data and refered to 1500 db. Isotachs are labeled in cm/sec; positive indicates south-southeastward flow, and negative (shaded part) north-northwestward flow.

3.2.3 A current measurement in the Kuroshio

by K. Takano, M. Okazaki and S. Imawaki

Three EG&G and two Aanderaa current meters were moored at Station MB (32°19.9'N, 134°01.6'E) in the Kuroshio 73 miles off Shikoku. Its twofold purpose is to get the vertical structure of the Kuroshio current from the intermediate layer down to the bottom layer, and to determine the depth of the reference level for the dynamic calculation of the geostrophic current.

The mooring is shown in Fig. 3.2.10. It was launched by the buoy first and anchor last method on Sep. 21.

Although the retrieval was initially scheduled for Oct. 5 fourteen days after the deployment, the operation was shifted one day ahead because of a typhoon coming nearer.

The command from the ship actuated one of two acoustic releases, which was told by the timed pinger from the release. The mooring did not get the sea surface, however, suggesting that mooring components should be entangled. A sweeping by a wire-rope caught its upper part but broke the nylon rope at a point marked by an arrow in Fig. 3.2.10. The upper part surfaced and was retrieved.

After finishing all the three legs, we stopped there on Oct. 25 en route to Tokyo to sweep the remaining lower part by the help of signals coming from the other acoustic release. It was fortunately caught by the sweeping nylon rope. With winding the sweeping rope, its tension was increased and signals from the release got nearer. A high tension of the rope around 2 tons is readily accounted for by the entanglement of

the release and anchor. The sweeping nylon rope was finally broken when we were winding it. The retrieval failed.

The analysis of the records from the retrieved current meters(one EG&G and two Aanderaas) is not yet completed. The upper Aanderaa gives an average velocity of 64.5 cm/sec towards 80° true at about 350 m depth and the lower Aanderaa gives an average velocity of 36.1 cm/sec towards 74° true at about 550 m depth, both with variations of about 12 hours period. The depths of the current meters are inferred from their water temperature records together with the vertical temperature profile obtained by both STD and XBT. The record from EG&G is almost not usable, probably due to mishandling of the film development in a commercial photo laboratory. However, some usable portion of it shows that the tilt of the current meter was more than 40° for a long period after the initial falling stage.

A numerical experiment on the mooring configuration using current speeds obtained by the two Aanderaa current meters shows that the mean overall tilt of the mooring line was 15°. The simulated mooring configuration gives the depths of the Aanderaa current meters compatible with the inferred depths(350 m and 550 m). The discrepancy between the tilt inferred from the numerical simulation and the tilt obtained by the EG&G current meter needs further consideration.

The current measurement, neither well defined nor well arranged, turns out a failure in this way.

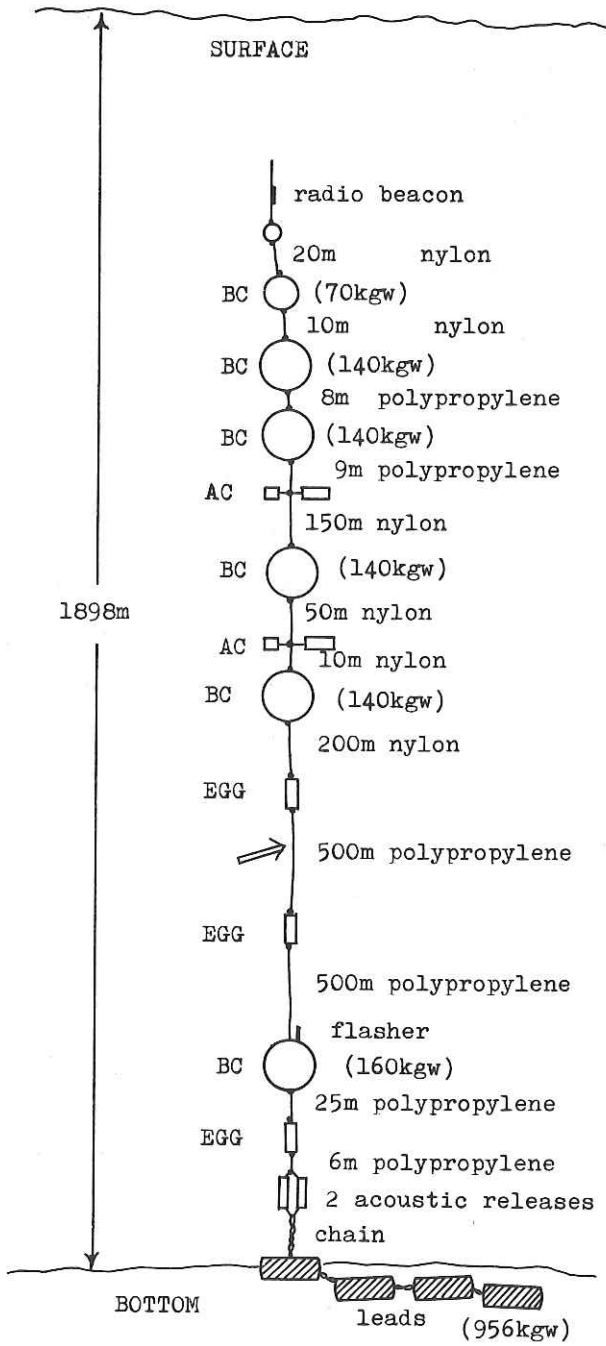

Fig. 3.2.10 Anticipated configuration of the mooring. AC and EGG denote Aanderaa and EG&G current meters, respectively. BC denotes a buoy cluster. Diameters of the plaited nylon rope and the plaited polypropylene rope are 16 mm and 20 mm, respectively.

3.2.4 Measurements of current and temperature at Sta. MA on the continental shelf off Tosa

by A. Maeda

The observation had been planned to examine the stochastic character of variations of current and temperature on the continental shelf off Tosa, Koochi Prefecture. Time scales in question were in a range from 20 minutes to a day. The Kuroshio current was flowing on the continental slope. Two current meters (MTCM-5) were moored at two depths about 15 m and 100 m from the bottom at Sta. MA (33°15.5'N, 133°38.8'E) on the shelf where the water depth was 195 m (Fig. 3.2.11). A temperature sensor was mounted on each current meter. We could not get records of current and temperature at 15 m from the bottom unfortunately, because of a damage to the case of the current meter at the depth. However, the another current meter satisfactorily operated. The measurement was made at intervals of 5 minutes from 22 Sep. to 6 Oct.. The records are shown in Fig. 3.2.12.

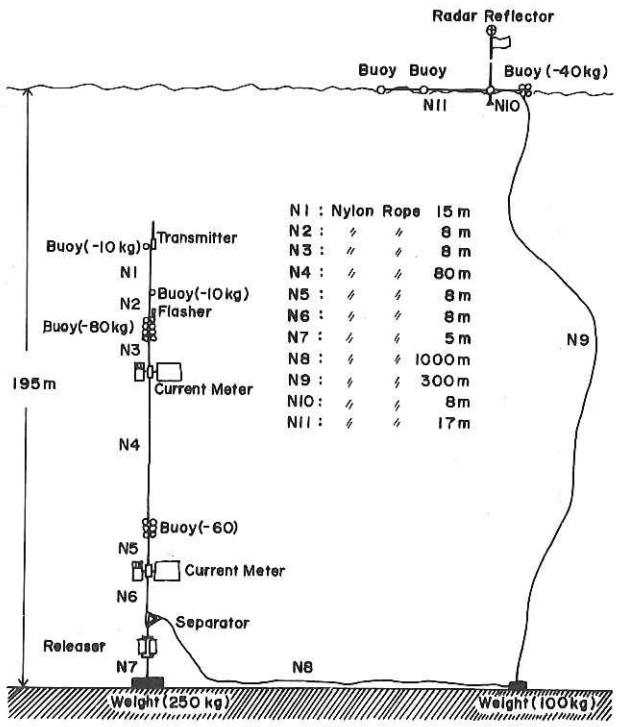

Fig. 3.2.11 Mooring of current meters.

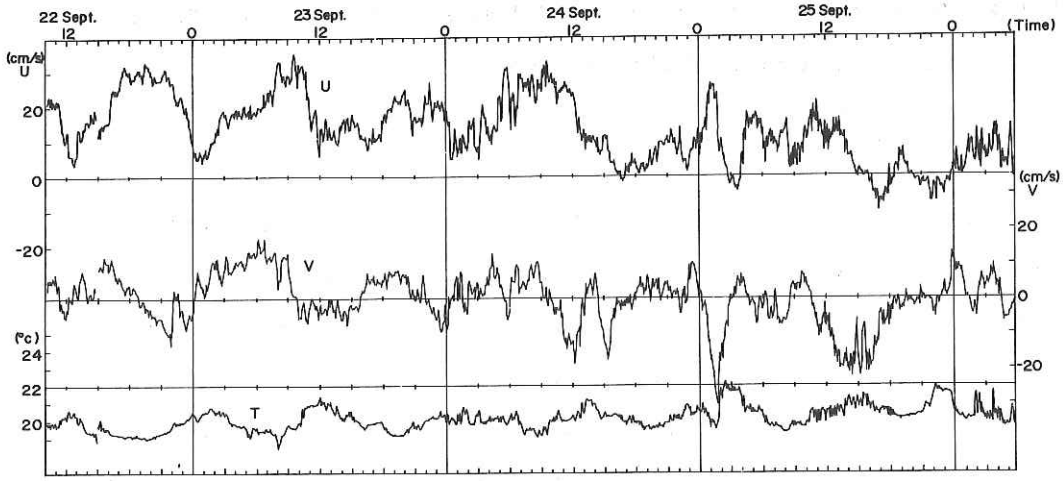

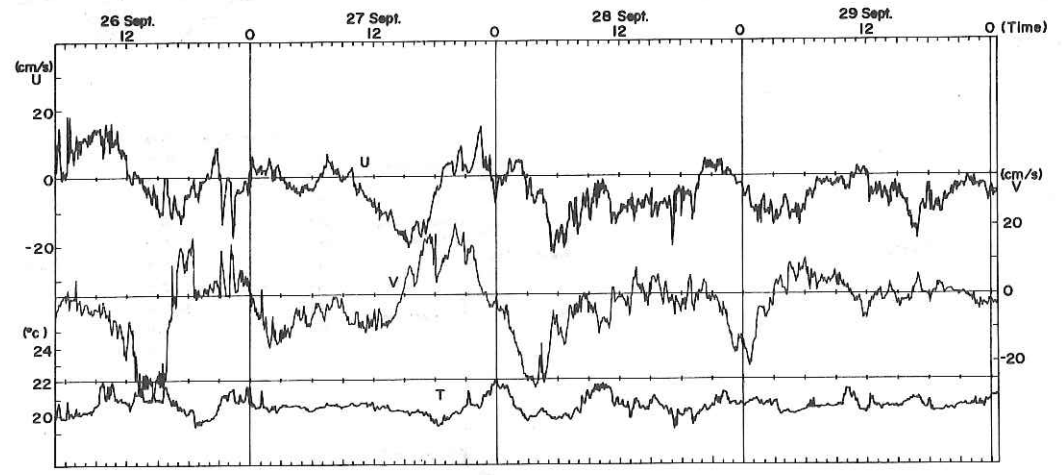

Fig. 3.2.12 Variations of current and temperature.
U: east-west component of current.
V: north-south component of current.
T: temperature.

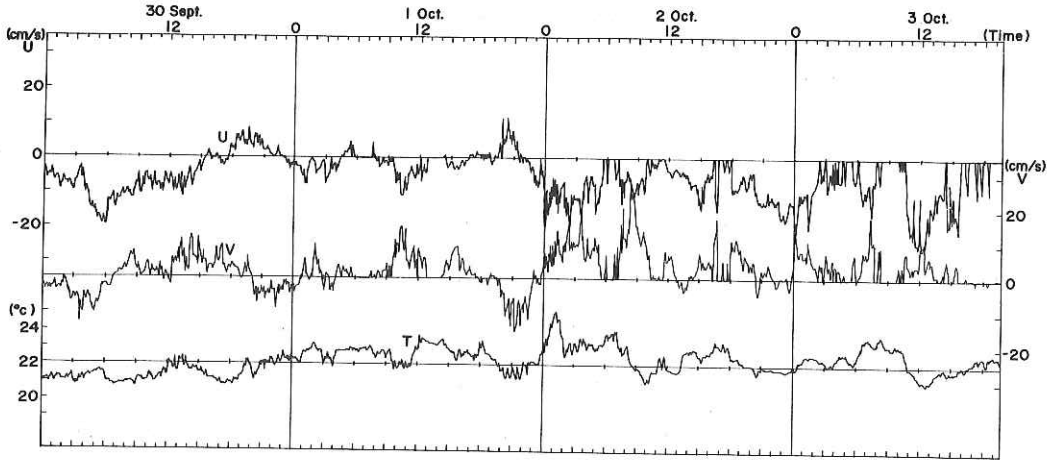
30 Sept.
12
0
1 Oct.
12
0
2 Oct.
12
0
3 Oct.
12
(Time)
(cm/s)
U
20
0
-20
U
V
(°c)
24
22
20
T
(cm/s)
V
20
0
-20

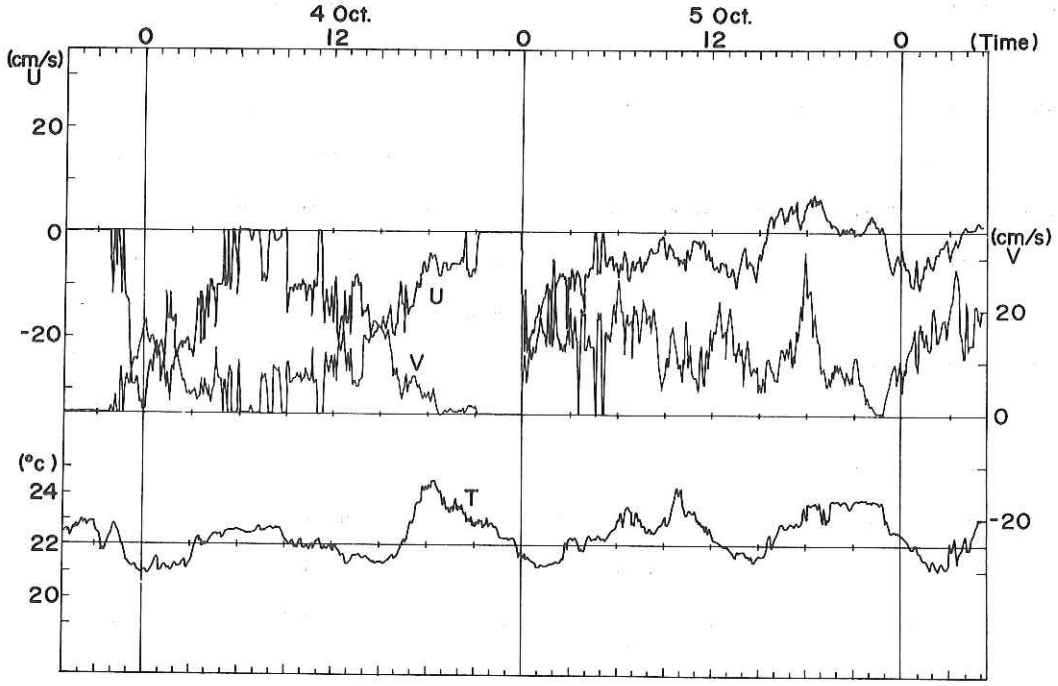
4 Oct.
12
0
5 Oct.
12
0
(Time)
(cm/s)
U
20
0
-20
U
V
(°c)
24
22
20
T
(cm/s)
V
20
0
-20

3.2.5 Study on quasi-absolute field of pressure

by H. Ishii, Y. Suzuki, M. Taniya and Y. Toba

1) Objective

To pursue possibility of forecasting oceanic variation is the final object of our investigation. Conventional observation which is usually performed is confined to structure of the upper ocean. However, there is a possibility that the absolute field of pressure or the absolute field of velocity is incorporated in oceanic variation such as large-scale meandering of the Kuroshio, although their accurate determination is difficult at present. However, if we assume that the total field of pressure in the open ocean is composed mainly of baroclinic component, it may be considered as a "quasi-absolute field of pressure". So, we have made an effort to determine the baroclinic field of pressure by observations of temperature, salinity and depth as accurate as possible from the bottom to the sea surface in the Kuroshio area. Our immediate plan is to compare such detailed baroclinic field of pressure with a conventional observation of the structure of the upper ocean, and to pursue some implications of it. At the same time, it is desired that current velocities estimated from dynamic calculation from data of the quasi-absolute field of pressure are compared with those obtained by direct current measurements by other research groups during the present cruise.

2) Observations

Serial observations have been carried out with Nansen bottles at nine stations on the SIK line and the MEN line, together with STD observations, the latter being performed from the sea surface to a 1500 m depth. In the serial

observations, Nansen bottles were casted in 14 or 15 layers from about 1300 m down to near the bottom. The temperatures have been read out up to 5/1000°C by reversing thermometers of 3°C range, and the salinity up to 1/1000 ‰ by an inductive salinometer, although the limit of confidence of measurements are 0.01°C and 0.003 ‰, respectively.

Based on these data, we have calculated the anomaly of specific volume δ ($= \alpha_{S,t,p} - \alpha_{35,0,p}$) and the anomaly of dynamic depth ΔD ($= \int_0^p \delta \, dp$).

3) Preliminary Results

In Fig. 3.2.13 is shown vertical distributions of δ at stations where Nansen casts were carried out the SIK line and MEN line. It is found that the gradient of δ among the neighbouring stations are significant even in the deep layer. Namely, the order of magnitude of the gradient is 10^{-1} Cl/ton km at near 1000-db surface, and decreases with depth to 10^{-2} Cl/ton km at 3000 db and 5×10^{-3} Cl/ton km at 3800 db.

The value of δ has a minimum near 3500-db surface, and increases downwards. The fact may be considered mainly as an adiabatic temperature variation by compression, since the potential density σ_θ increases monotonously without maximum, and attains a constant value, which is also horizontally homogeneous, in sufficiently deep layer. Temperature sections also show a minimum layer at about 3500-m depth, and slight rising of temperature downwards.

Acknowledgement

We would like to take this opportunity to extend our many thanks to all people who were concerned in and helped our present work. Our special thanks are due to Mr. S.Kurashina and members of the Oceanog. Div., Hydrogra. Dept. of Japan, for their kind help in the use of reversing thermometers for deep-sea use.

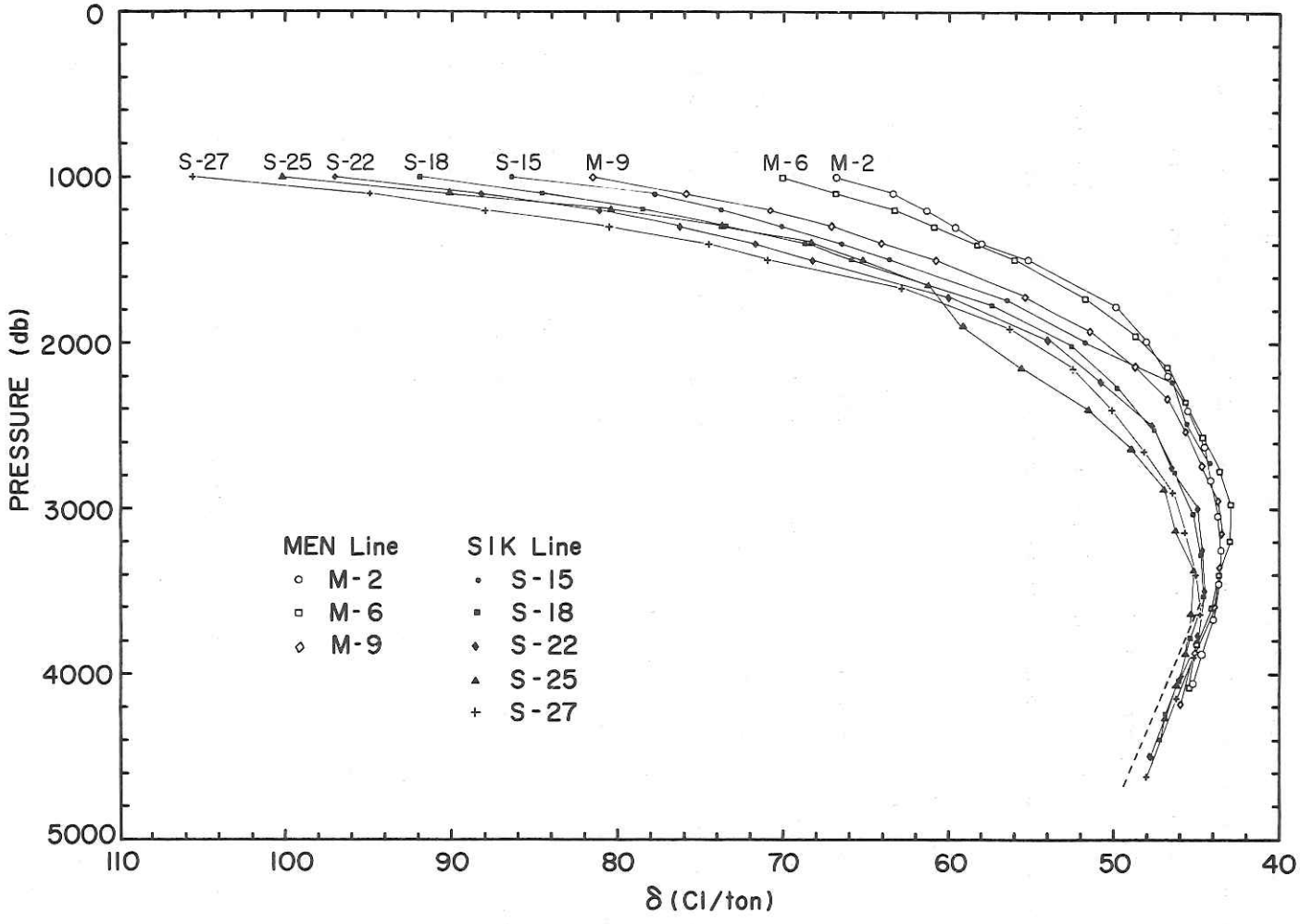

Fig. 3.2.13 Vertical distributions of the anomaly of the specific volume δ at stations where Nansen casts were carried out. Broken line shows relation for adiabatic temperature variation.

3.3 Leg III Observations of detailed oceanic structure near the shoal Kokusho-sone

by N. Nagata and M. Fukasawa

In Leg III, the detailed oceanic structure was observed near the shoal Kokusho-sone (30°00'N, 128°30'E), which is located near the axis of the Kuroshio in the East China Sea.

The observation lines are shown in Fig. 3.3.1; o indicates the STD stations, x the XBT stations and the solid line the dense XBT observation line. A water mass analysis was made by adopting the conventional demarcation of water types after Yoichi Hanzawa, Nagasaki Marine Observatory, JMA. Demarcation of water types is shown in Fig. 3.3.2; water type K is the Kuroshio water and I, II, III and IV are the mixed waters between coastal and Kuroshio waters where an increase in the Roman numeral indicates an increase of the influence of the coastal water. The results are shown in Figs. 3.3.3 through 3.3.6. The mixed coastal waters are arranged in complicated patterns in all cross-sections, and seem to indicate that complicated mixing processes take place between the coastal and Kuroshio waters.

The detailed temperature cross-section along the meridian of 128°30'E which passes on the shoal Kokusho-sone (Line B) is shown in Fig.3.3.7. The position of the shoal was well inside of the sharp southward gradient of the isotherms which corresponds to the current zone of the Kuroshio. At depths from 150 m to 280 m, a prominent uplifting of isotherms having a horizontal scale of several miles is seen just north of the shoal position. At depths from 280 m to 350 m, the temperature difference can be seen across the shoal. These patterns suggest that forced upwelling takes place along the north slope of the shoal.

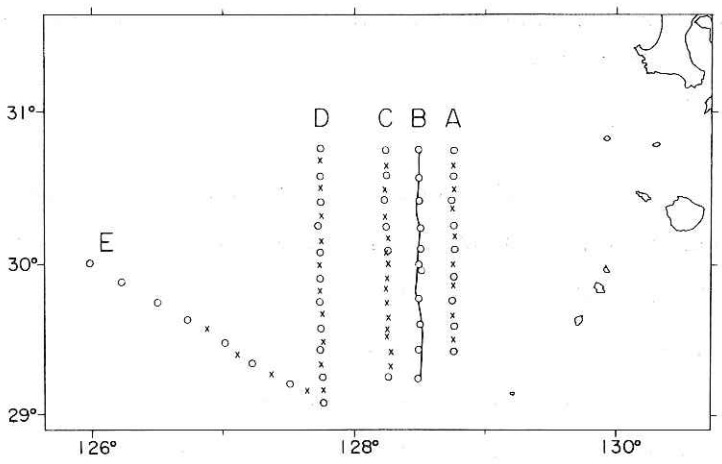

Fig. 3.3.1

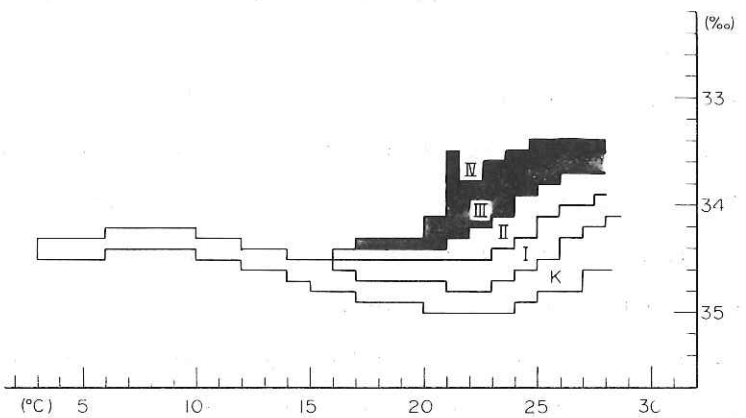

Fig. 3.3.2

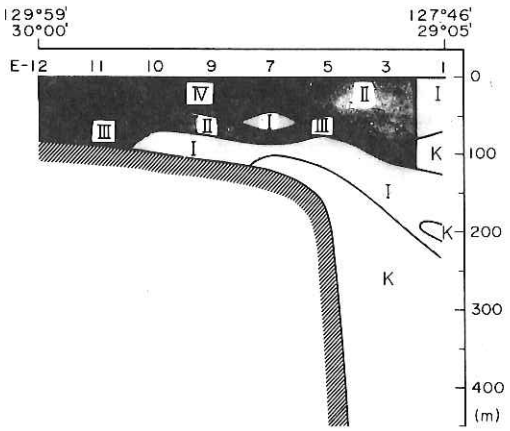

Fig. 3.3.3

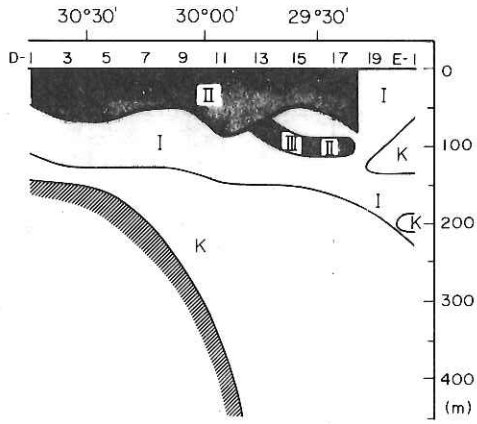

Fig. 3.3.4

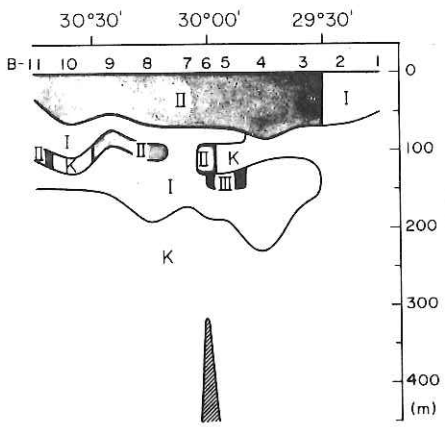

Fig. 3.3.5

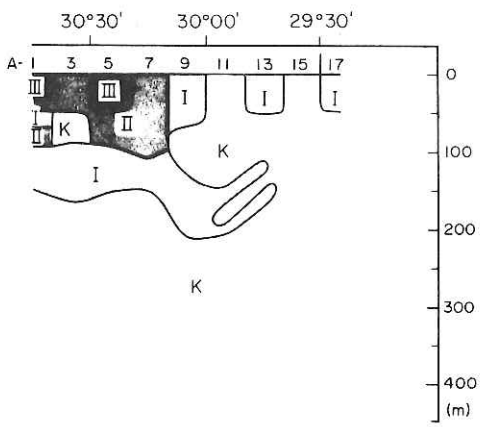

Fig. 3.3.6

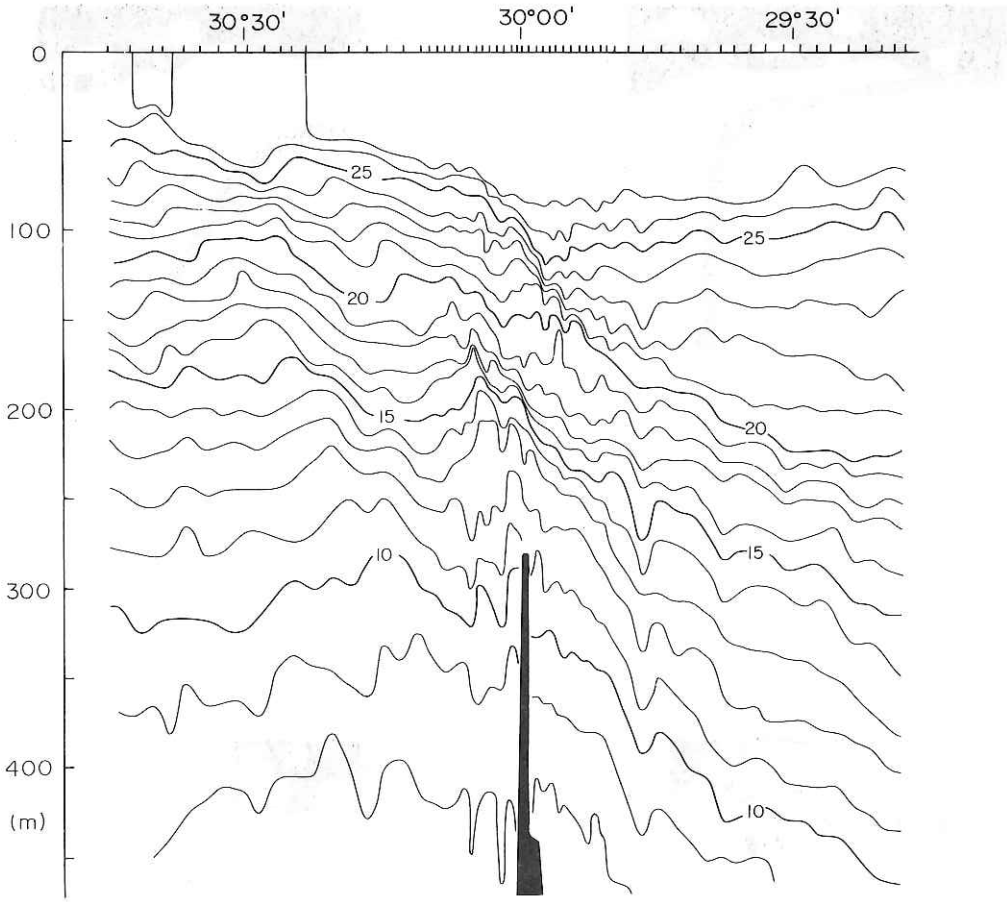

Fig. 3.3.7

3.4 Leg IV Other observations

3.4.1 Beam attenuation coefficient and particle size distribution

by K. Matsuike and T. Morinaga

During the Leg II, which traversed the Kuroshio in two different locations, the beam attenuation was measured at many positions to determine the optical structure of the Kuroshio as well as the structure of the front between the Kuroshio and coastal water from the viewpoint of optical characteristics. Particle sizes were also measured to determine their distribution from the surface to the depth of 3500 m at some locations. These measurements were made simultaneously with other measurements of temperatures, salinities and current velocities.

A submarine instrument for the measurement of beam transmittance is the in-situ transmissometer (Model XMS, Martek Co. Ltd.). The instrument provides a path length of 1 meter and is equipped with a wratten filter (No. 45) to give blue light transmittance at the peak wave length of 493 nm; the medium wave length is 486 nm, and the bandpass (50% points) is 53 nm, respectively. A Coulter Counter (Model ZBI, Coulter Electronics Co. Ltd.) was used to measure suspended particles of sizes not less than 1μ.

The distributions of beam attenuation coefficient α at four cross sections are presented in Fig. 3.4.1 to 3.4.4. Fig. 3.4.5 and 3.4.6 are distributions of particle sizes and particle cross-section concentrations at Sta. S-7.

The results of the survey are summarized as follows,

1) A turbid water layer having a thickness of about 20 meters was observed at depths of 50 to 60 meters in the Kuroshio. This

turbid water mass joins with turbid coastal water when the Kuroshio approaches near to the coast of Japan. It was found that these two water masses, coastal and Kuroshio waters, had equal in-situ density. This feature is considered to offer a valuable suggestion regarding the motion of water at the front between these different water masses.

2) The beam attenuation coefficient in the Kuroshio remains approximately constant regardless of time and position, exhibiting a constant value of 0.11 m^{-1} to 0.12 m^{-1} (486 nm). This provides a useful criterion for comparing the extent of attenuation in other water masses.

3) In a specific water mass of the Kuroshio in which turbidity retains a very stable value, the concentration of suspended particles is 0.18 ppm and their average diameter is 1.27 μ. In every water area covered by this survey, the particle volume in layers deeper than 50 meters decreased with depth. The particle concentration was 0.01 ppm at the depth of 500 meters and then, it scarcely changed down to the depth of 3500 meters.

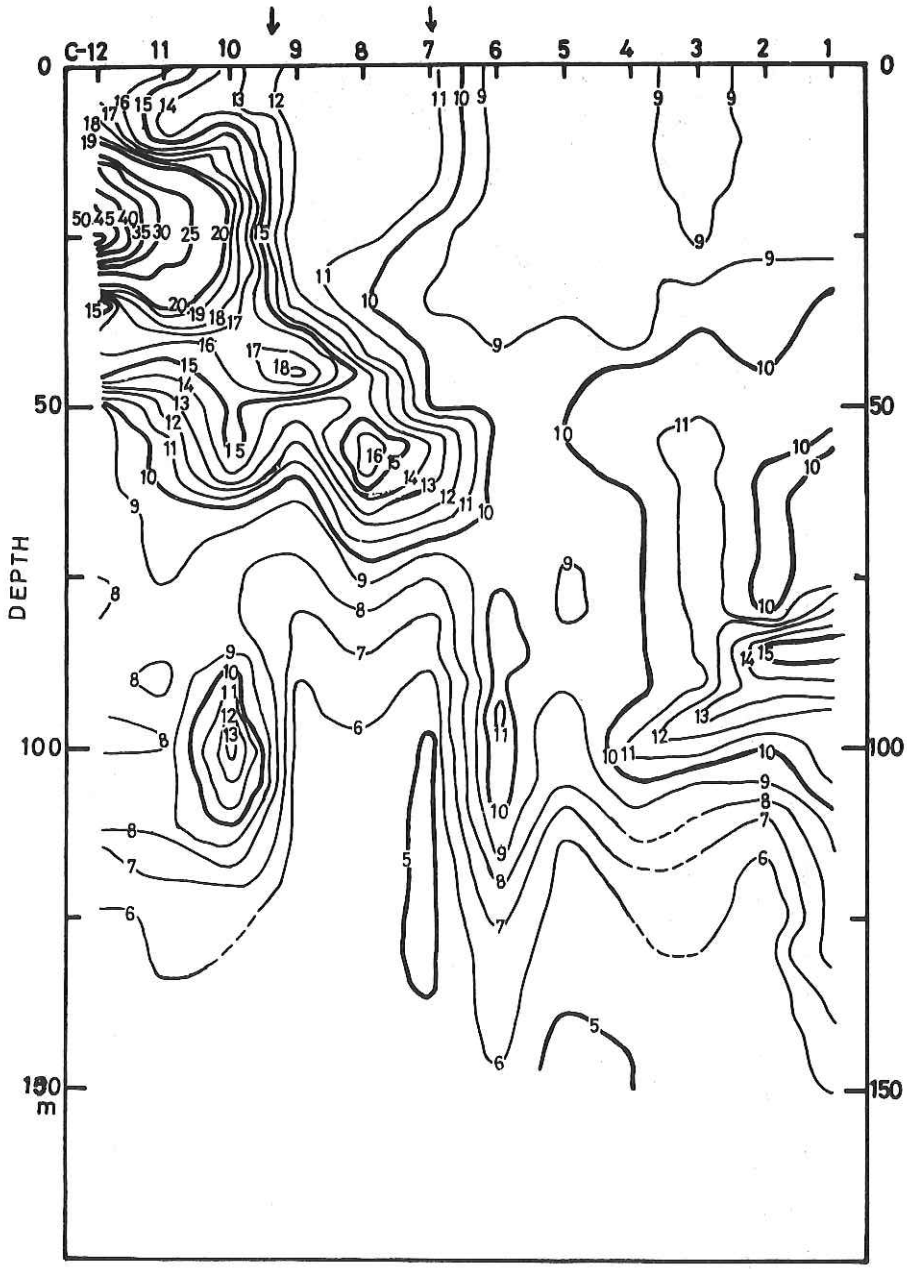

Fig. 3.4.1 Vertical profile of beam attenuation coefficient, α, from Sta. C-1 to Sta. C-12. As for position of these stations, refer to Fig. 3.2.1. The Section-C almost coincides with a part of the Section-SIK. Sta. C-1 is in the vicinity of S-19 and Sta. C-12 in the vicinity of S-6. Figures on iso-lines denote values of $\alpha \times 10^{2} m^{-1}$. Arrows show the northern and the southern boundary of the Kuroshio area with a current speed of 1.5 knots or more.

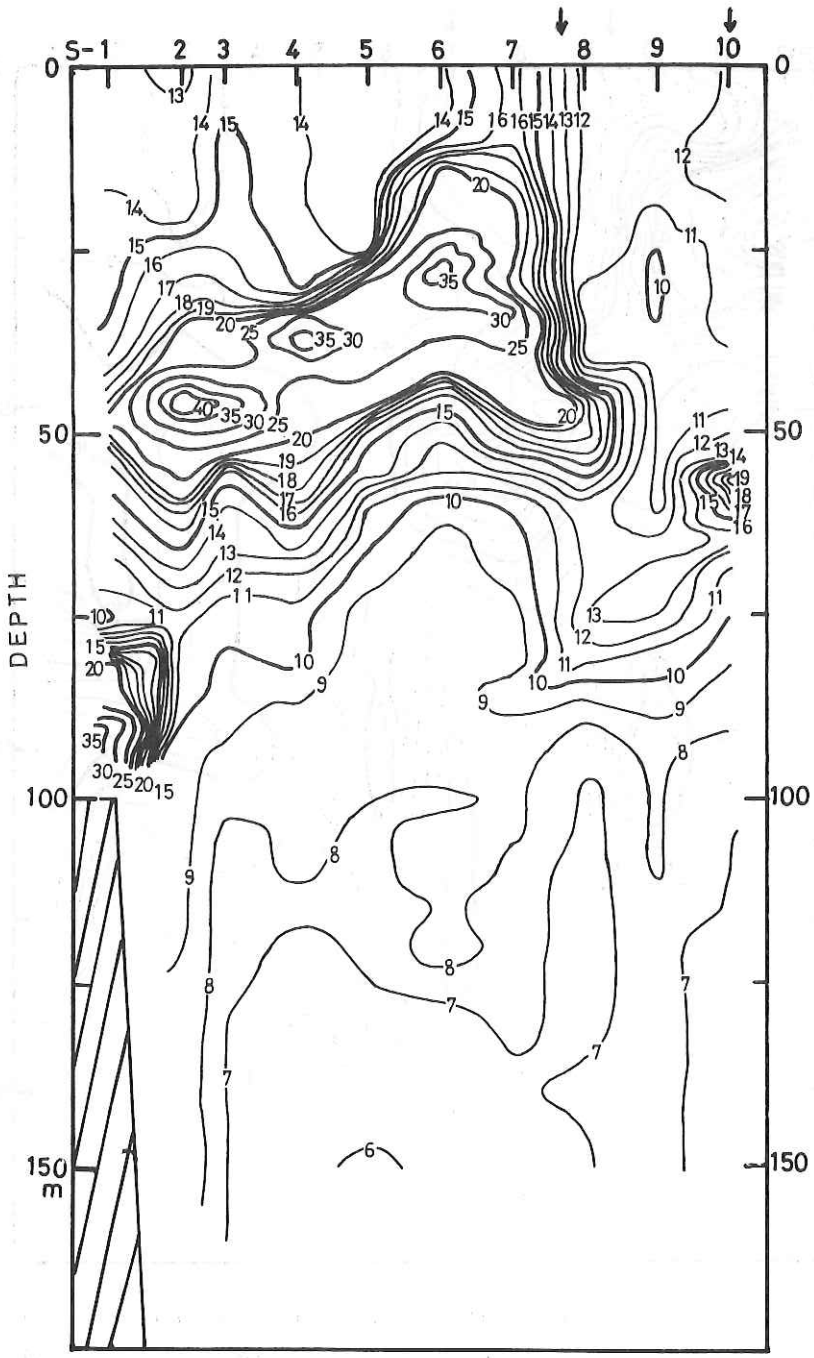

Fig. 3.4.2 Vertical profile of beam attenuation coefficient, α, from Sta. S-1 to Sta. S-10. As for positions of these stations, refer to Fig. 3.2.1. Figures on iso-lines denote values of $\alpha \times 10^{2} m^{-1}$. Arrows show the northern and the southern boundary of the Kuroshio area with a current speed of 1.5 knots or more.

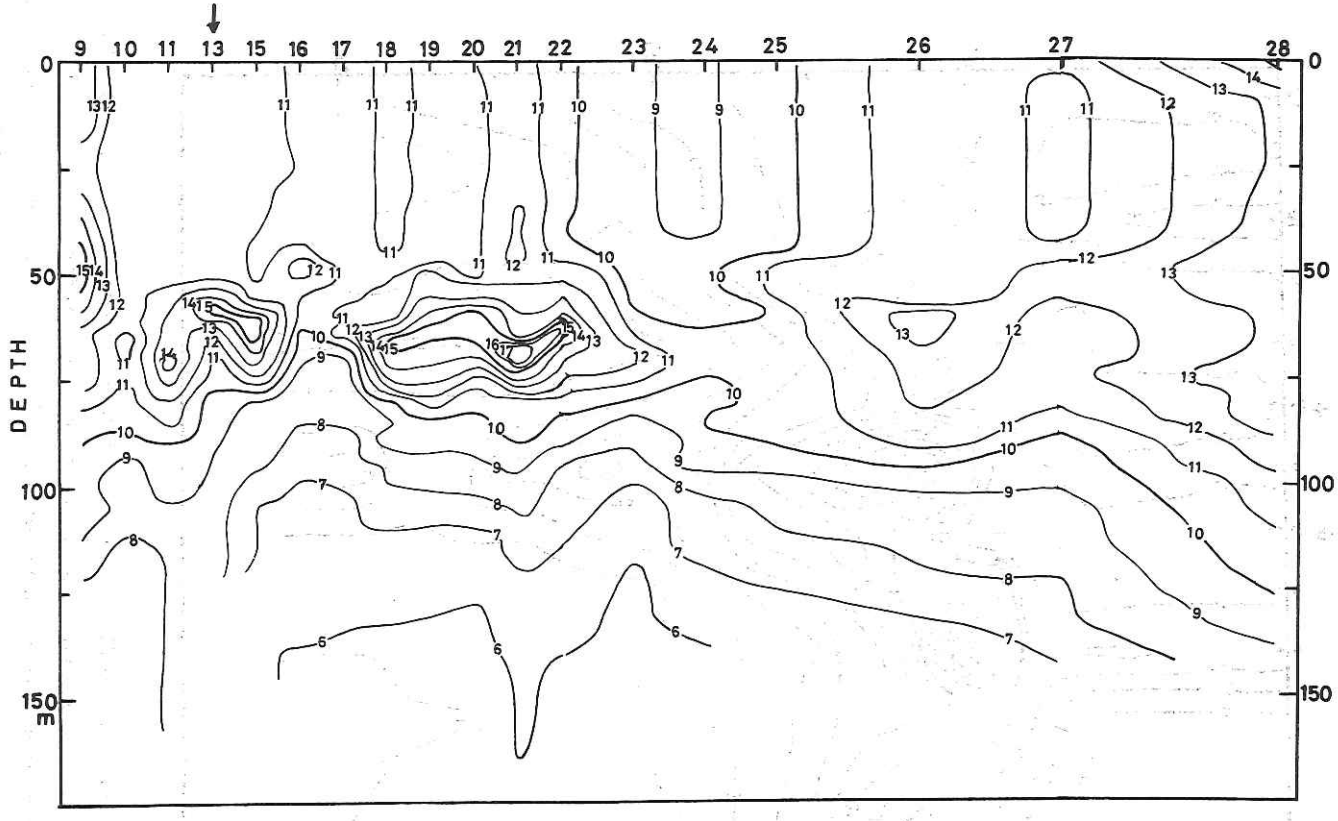

Fig. 3.4.3 Vertical profile of beam attenuation coefficient, α, from Sta. S-9 to Sta. S-28. As for positions of these stations, refer to Fig. 3.2.1. Figures on iso-lines denote values of $\alpha \times 10^{2}$ m^{-1}. An arrow shows the southern boundary of the Kuroshio area with a current speed of 1.5 knots or more.

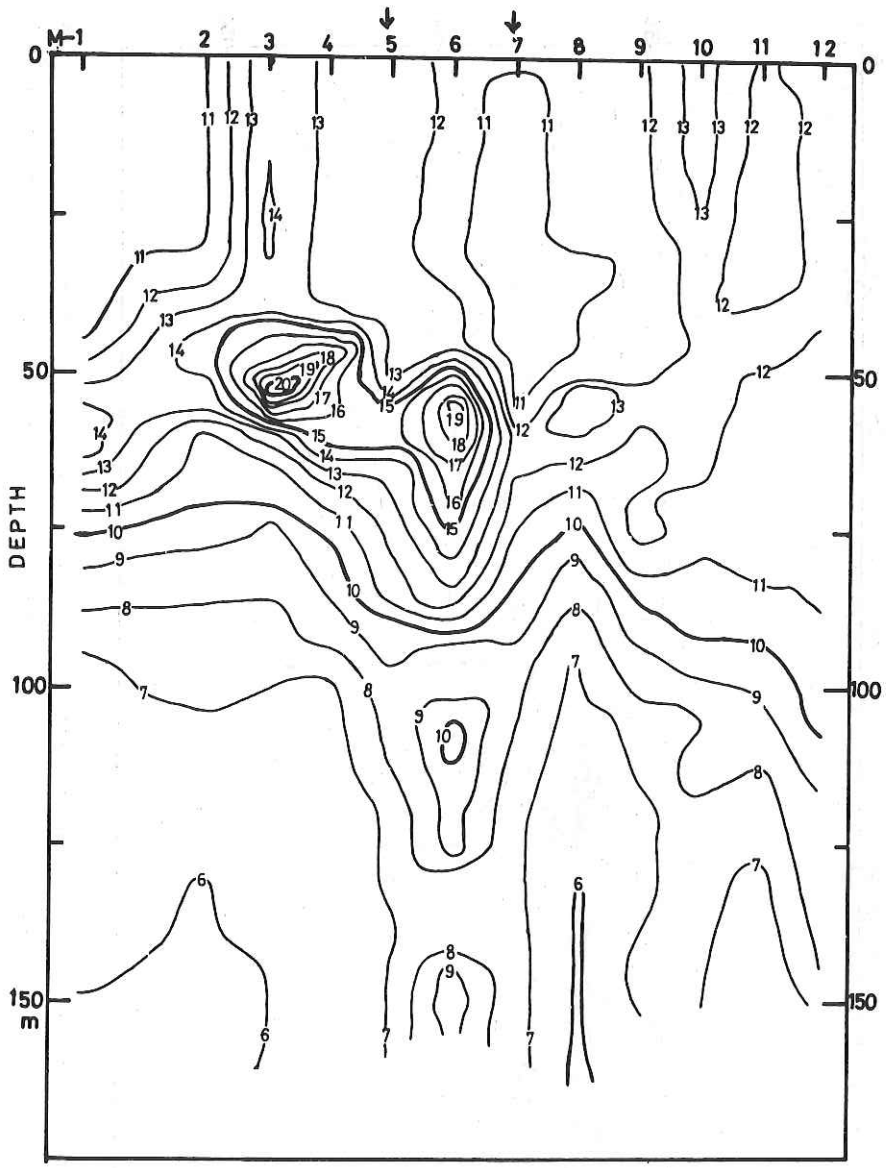

Fig. 3.4.4 Vertical profile of beam attenuation coefficient, α, from Sta. M-1 to Sta. M-12. As for positions of these stations, refer to Fig. 3.2.1. Figures on iso-lines denote values of $\alpha \times 10^{2} m^{-1}$. Arrows show the eastern and the western boundary of the Kuroshio area with a current speed of 1.5 knots or more.

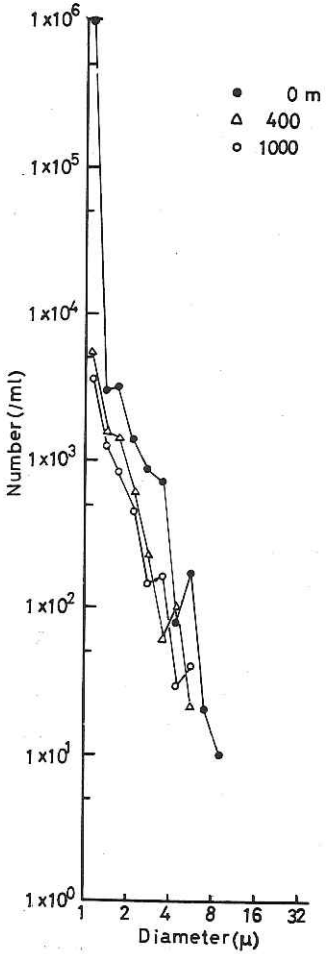

Fig. 3.4.5 Particle size distribution at the surface and at the depths of 400 m and 1000 m at Sta. S-7.

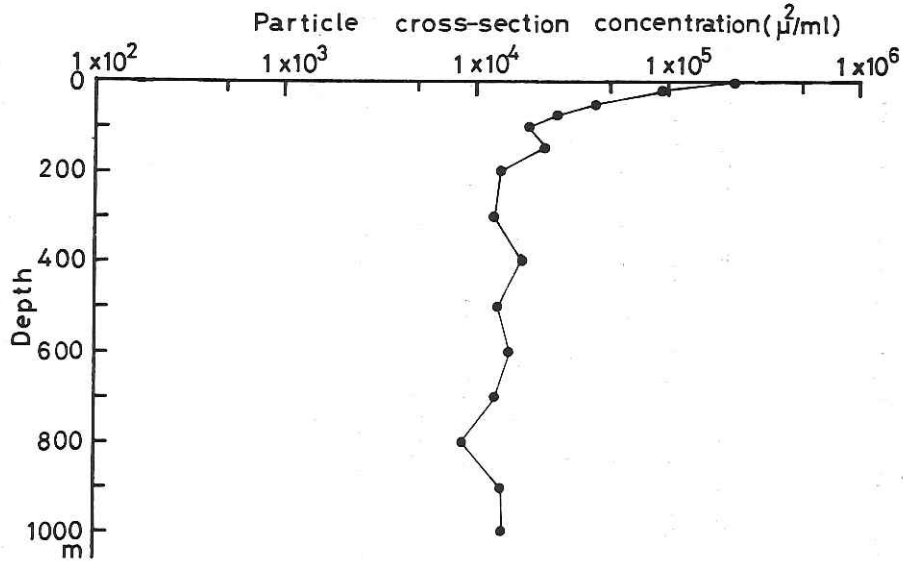

Fig. 3.4.6 Vertical distribution of the cross-section concentration of particles at Sta. S-7.

3.4.2 Measurements of turbulent heat flux in the Kuroshio region

by M. Sakurai

By use of the bulk method, fluxes of momentum, sensible and latent heats are estimated from measurements of wind speed, U, temperature difference between sea surface and air, Tw-T, and sensible humidity difference between sea surface and air, qw-q. The measurements were made in the Kuroshio region during the period from September 15th to October 6th. The measurement of specific humidity was made with an Assman psychrometer. Fluxes of momentum, sensible and latent heats together with specific humidity are plotted in Fig. 3.4.7. Formulae used for the estimations are as follows.

$\tau = \rho a C d U^2$,

$H = \rho a C p C h U (Tw-T)$,

$L = \rho a C L U (qw-q)$,

where

τ: momentum flux, H: sensible heat flux, L: latent heat flux,

ρa: air density, U: wind speed, Cd: drag coefficient of wind,

Cp: specific heat at constant pressure of air,

Ch: Stanton number, CL: Dalton number.

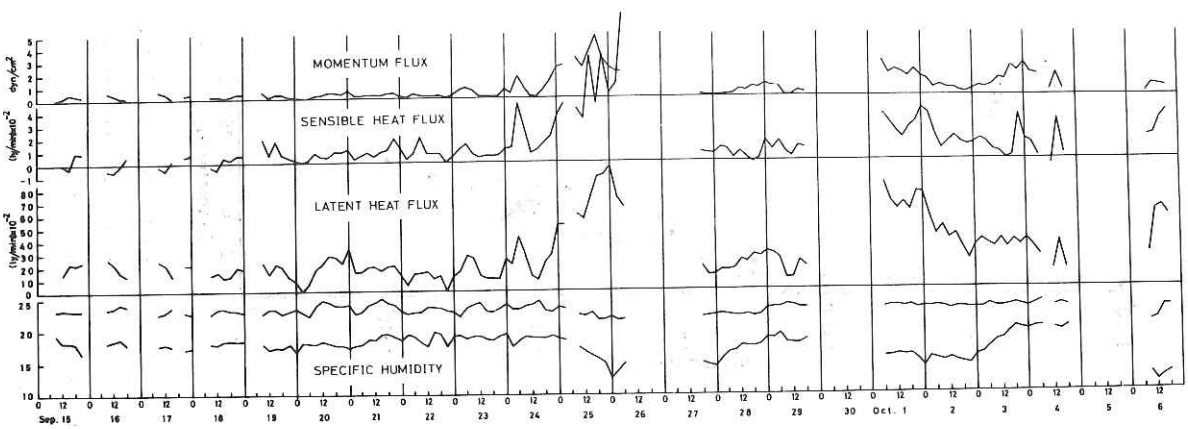

Fig. 3.4.7

3.4.3 Inorganic nitrogen metabolism in the East China Sea

by T. Saino and A. Hattori

Uptake of inorganic nitrogenous compounds by phytoplankton was measured using a ^{15}N tracer technique. The fixation of molecular nitrogen was determined by an acetylene reduction technique.

Surface waters collected at 6 stations (Table 3.4.1) were filtered through net cloth (0.33 mm mesh) immediately after sampling, and introduced into 500 ml glass bottles for ^{15}N uptake measurement or into 5 litre glass bottles for acetylene reduction.

Effects of concentration of ammonia or nitrate on their uptake were examined. Incubation was conducted under the following conditions: ^{15}N-ammonia or nitrate, 0.1-10 µg atom N/l; temperature, 25-26°C; light intensity, 14,000 lux or in darkness; incubation time, 3 hrs.

Acetylene gas (product of Matheson Co.) was introduced into 1 litre of gas space to yield its partial pressure of 0.1 atmosphere. The bottles were incubated in a deck incubator cooled by surface water under natural sunlight. At intervals, aliquots of gas were withdrawn with vacutainers. Production of ethylene was later determined by a Shimazu GC-4 gaschromatograph.

Solar irradiance was measured continuously with an underwater irradiance meter.

Aliquots of seawater samples were filtered through a Whatman type C glass fibre filter. The filters with residue and the filtrates were stored in frozen state for later determinations of chlorophyll content and nutrients, respectively.

Table 3.4.1

Location of sampling stations

Date	Longitude	Latitude
14 Oct.	128°45.9'E	30°05.7'N
15 Oct.	128 30.5	30 06.7
16 Oct.	128 14.9	29 52.0
17 Oct.	127 44.4	29 26.2
18 Oct.	125 59.0	30 00.5
24 Oct.	130 08.5	29 02.5

3.4.4 Study on phytoplankton

by T. Nakai, T. Ishimaru and R. Marumo

For the study on taxonomy and distribution of coccolithophorids and other phytoplankton in relation to environmental factors, 500 ml of sea water were collected at 103 stations. Organisms in these samples were fixed by neutralized formalin and filtered with Millipore filter HA. Microscopical examinations are now in progress.